

**Role of Class III Peroxidase PRX34 in Plant  
Oxidative Burst and Immunity**

**March 2019**

**LEI ZHAO**

**The Graduate School of Environmental and Life Science  
(Doctor's Course)**

**OKAYAMA UNIVERSITY, JAPAN**



# CONTENTS

<b>CHAPTER I</b>	1
<b>General Introduction</b>	1
<b>1.1 Molecular mechanisms of plant-pathogen interactions</b>	2
<b>1.2 Reactive oxygen species in plant signaling</b>	3
<b>1.3 RBOH/NADPH oxidase</b>	5
<b>1.4 Apoplastic class III peroxidase</b>	7
<b>1.5 Purposes of the study</b>	10
<b>CHAPTER II</b>	11
<b>Some T-DNA Insertion Lines that Affect the Expression of <i>PRX34</i></b>	11
<b>2.1. Abstract</b>	12
<b>2.2 Introduction</b>	12
<b>2.3 Materials and Methods</b>	15
2.3.1 Plant Materials and Growth Conditions	15
2.3.2 RNA Extraction and Quantitative RT-PCR Analysis	20
2.3.4 Cell Wall Proteins Extraction	21
2.3.5 Detection of PRX34 Corresponding Peroxidase by Immunoblotting	22
2.3.6 Statistical Analysis	22
<b>2.4 Results</b>	22
2.4.1 Identification of <i>prx34</i> T-DNA mutants	22
2.4.2 <i>prx34-2</i> and <i>pr34x-3</i> mutations impaired in accumulation of corresponding peroxidase	25
<b>2.5 Discussion</b>	27

<b>Chapter III</b>	29
<b>Peroxidase Knockout Lines are Compromised in Flg22-Elicited Immune Responses</b>	29
<b>3.1 Abstract</b>	30
<b>3.2 Introduction</b>	30
3.2.1 <i>Botrytis cinerea</i>	30
3.2.2 <i>Pectobacterium carotovorum</i>	31
3.2.3 <i>Colletotrichum higginsianum</i>	32
3.2.4 Callose	33
<b>3.3 Materials and Methods</b>	35
3.3.1 Plant Materials and Growth Conditions	35
3.3.2 Infection Assays	35
3.3.3 Assay for Callose Formation	36
3.3.4 Detection of Reactive Oxygen Species	37
<b>3.4 Results</b>	38
3.4.1 <i>prx34-2</i> and <i>prx34-3</i> mutant plants exhibit enhanced susceptibility to <i>B. cinerea</i> , <i>C. higginsianum</i> and <i>P. carotovorum</i> subsp. <i>carotovorum</i>	38
3.4.2 <i>prx34-2</i> and <i>prx34-3</i> mutations are compromised in Flg22-elicited immune responses	41
<b>3.5 Discussion</b>	46
<b>Chapter IV</b>	47
<b>Overexpression of <i>PRX34</i> Enhance Flg22-elicited Immune Responses and Confers Resistance to Pathogens</b>	47
<b>4.1 Abstract</b>	48
<b>4.2 Introduction</b>	49
4.2.1 <i>Pseudomonas syringae</i> pv. <i>tomato</i> strain DC3000	49
4.2.2 Luminol L-012	50
<b>4.3 Materials and Methods</b>	51

4.3.1 Plant Materials and Growth Conditions	51
4.3.2 RNA Extraction and Quantitative RT-PCR Analysis	51
4.3.3 Infection Assays	51
4.3.4 Detection of Reactive Oxygen Species	52
4.3.5 Assay for Callose Formation	52
4.3.6 Chemiluminescence detection of the oxidative burst in plant leaf pieces	52
<b>4.4 Results</b>	<b>53</b>
4.4.1 Identification of two independent <i>35S:PRX34</i> -overexpressing lines	53
4.4.2 Overexpression of <i>PRX34</i> confers resistance to virulent strains <i>B. cinerea</i> , <i>P. carotovorum</i> subsp. <i>carotovorum</i> and <i>Pseudomonas syringae</i> pv. <i>tomato</i>	55
4.4.3 Overexpression of <i>PRX34</i> are enhanced in Flg22-elicited immune responses	57
4.4.4 Detection of the ROS-burst in plant leaf pieces using a luminol-based bioassay	60
<b>4.5 Discussion</b>	<b>62</b>
<b>SUMMARY</b>	<b>64</b>
<b>REFERENCES</b>	<b>65</b>
<b>Acknowledgements</b>	<b>82</b>

# LIST OF FIGURES

Number	Title	Page
Figure 2.1	Gene organization of <i>AtPRX34</i> ( <i>At3g49120</i> ) and insertion sites of T-DNA	16
Figure 2.2	Genotyping for three <i>prx34</i> mutants	18
Figure 2.3	Phenotypic and molecular characterization of <i>atprx34</i> mutants	24
Figure 2.4	Reduced ROS generation and decreased peroxidase activity in <i>prx34-2</i> and <i>prx34-3</i> mutants	26
Figure 3.1	Enhanced susceptibility of <i>prx34</i> mutants to fungal and bacterial pathogens	39
Figure 3.2	Response of <i>prx34-1</i> mutants to fungal and bacterial pathogens	40
Figure 3.3	Response of <i>prx34-1</i> and <i>prx34-2</i> mutants to Flg22	42
Figure 3.4	Response of <i>prx32</i> and <i>prx34-1</i> mutants to Flg22.	44
Figure 4.1	Characterization of <i>35S:PRX34</i> overexpression line in <i>Arabidopsis thaliana</i> (Col)	54
Figure 4.2	Overexpression of <i>PRX34</i> caused enhanced resistance to virulent strains of fungal and bacterial pathogens	56
Figure 4.3	Detection of <i>PRX34</i> -overexpression lines in response to Flg22	58
Figure 4.4	Kinetic analysis of ROS generated in the wild-type and the OX #8-1 in the absence or presence of diphenylene iodonium (DPI), a chemical inhibitor of NADPH oxidase	61
Figure 5	Induction of <i>PRX34</i> transcript levels in <i>Arabidopsis</i> in response to Flg22 or chitoheptaose	63

# **CHAPTER I**

## **General Introduction**

## **1.1 Molecular mechanisms of plant-pathogen interactions**

Plants have established a complicated immune defense system during co-evolution with pathogens. The innate immune system of plants can be generally divided into two levels (Jones and Dangl, 2006). The first active layer of the plant immune system is the recognition of pathogen-associated molecular patterns (PAMPs) (Bittel and Robatzek, 2007; Zipfel, 2008, 2009). PAMPs are detected by highly conserved PRRs that contain an extracellular leucine-rich repeat domain and an intracellular kinase domain, and these subtly different yet exquisitely conserved PRRs have now been characterized in rice (Ito et al. 1997; Lee et al. 2009; Schwessinger and Ronald 2012; Song et al. 1995), fruit flies (Lemaitre et al. 1996), humans (Kirschning et al. 1998; Medzhitov et al. 1997), mice (Poltorak et al. 1998), and Arabidopsis (Gomez-Gomez and Boller 2000; Schwessinger and Zipfel 2008; Zipfel et al. 2006). PAMPs are typically conserved molecules characteristic to a whole class of microbes and include for example fungal chitin and microbe-derived structures like bacterial flagellin, EF-Tu or their peptide surrogates Flg22 and Elf18, respectively (Jones and Dangl, 2006; Zipfel, 2008). PAMPs can also be associated with non-pathogens and referred to as microbe-associated molecular patterns (MAMPs) (Zipfel, 2008). In addition to recognition of PAMPs, plants have the ability to recognize modified-self, including damage-associated molecular patterns (DAMPs) (Ferrari et al., 2013). A major category of DAMPs are plant cell-wall fragments released by the action of plant cell-wall degrading enzymes (PCWDEs) secreted by necrotrophic and hemibiotrophic pathogens. Pectin is a central component in plant cell walls and constitute a major target for PCWDEs

during pathogen invasion. Oligogalacturonide (OG) fragments of pectin released by the action of pectin degrading enzymes such as polygalacturonases (PGs) are the best characterized plant DAMPs that activate innate immune responses (Ferrari et al., 2013; Bellincampi et al., 2014). The recognition of PAMPs and DAMPs leads to the activation of plant defenses and pattern-triggered immunity (PTI), which provide resistance to most non-adapted pathogens in a phenomenon called non-host resistance (Zipfel, 2009, 2014).

The other active layer begins in cytoplasm and mainly relies on recognition of microbial effectors by plant resistance proteins in direct or indirect ways, which then initiates potent defense responses (Zipfel, 2014). This process, termed effector-triggered immunity (ETI), a rapid response that amplifies PTI signaling events and limits pathogen spread (Dangl et al., 2013), is necessary for defense against pathogens that can secrete effectors to suppress the first level of immunity. Activation of these two layers of immunity in plant is based on distinguishing and recognition of “self” and “non-self” signals. Recognition of “non-self” signals can activate signal cascades, such as MAPK cascades, which will then induce defense gene expression and corresponding defense responses.

## **1.2 Reactive oxygen species in plant signaling**

According to current knowledge, recognition of PAMPs, DAMPs and effectors triggers overlapping signaling responses in the plant and indicate a difference in the speed, persistence and robustness rather than the quality of response between PTI and

ETI (Espinosa and Alfano, 2004; Tsuda and Katagiri, 2010). Both layers of the immune response share many signaling elements (Dodds and Rathjen, 2010). Among these, apoplastic production of reactive oxygen species (ROS) is one of the fastest physiological responses ubiquitously observed in plants after pathogens are recognized by PRRs (Macho and Zipfel, 2014), or by resistance proteins during ETI. The rapid accumulation of ROS after pathogen recognition is commonly referred to as the oxidative burst (Baker and Orlandi 1995; Bolwell et al. 2002; Mehdy 1994; Sutherland 1991), and is accompanied by changes in extracellular pH, ion fluxes, protein phosphorylation and immobilization (Bolwell et al. 1995; Davies et al. 2006; Felix et al. 1993; Wojtaszek et al. 1995). ROS has been implicated not only in direct antimicrobial roles (Peng and Kuc 1992), but also in cellular signalling associated with the induction of defence gene expression (Desikan et al. 2000), the hypersensitive response (HR) (Lamb and Dixon 1997; Thordal-Christensen et al. 1997), cell wall protein cross-linking (Brown et al. 1998), phytoalexin production (Apostol et al. 1989; Daudi et al. 2012; Devlin and Gustine 1992; O'Brien et al. 2012; Qiu et al. 2012), callose deposition (Daudi et al. 2012; O'Brien et al. 2012) and systemic acquired resistance (SAR) (Alvarez et al. 1998; Lamb and Dixon 1997).

The evolution of multicellular life forms has been shaped by the oxygen-rich atmosphere (Raymond J and Segré D, 2006). In the presence of oxygen, cellular processes characterized by high rates of electron or energy transfer inevitably lead to the formation of reactive oxygen species (ROS) by electron or energy leakage to molecular oxygen (O<sub>2</sub>). Additionally, multiple enzymatic reactions have evolved to

produce ROS either as a primary product or as a by-product. ROS are defined as oxygen-containing molecules exhibiting higher chemical reactivity than O<sub>2</sub>. In plants, the major forms of ROS are singlet oxygen (<sup>1</sup>O<sub>2</sub>), superoxide anion (O<sub>2</sub><sup>•-</sup>), hydrogen peroxide (H<sub>2</sub>O<sub>2</sub>), and hydroxyl radical (HO<sup>•</sup>). The potential for cellular damage from enhanced production of these molecules has been alleviated through evolutionary pressure to develop and expand a range of enzymatic and nonenzymatic ROS scavengers. Rapid changes in compartmental redox balance and ROS homeostasis are among the earliest symptoms following fluctuations in environmental conditions. Plants monitor these parameters and utilize them as signals in multiple processes that serve to adjust metabolism or physiology either at the whole plant or tissue level or in specific subcellular compartments. During most abiotic and biotic stress responses, plasma membrane-localized NADPH/NADH oxidases and cell wall-localized class III (CIII) apoplastic peroxidases are the major sources of ROS (Grant et al., 2000; Bolwell et al., 2002).

### **1.3 RBOH/NADPH oxidase**

NADPH oxidases have been implicated in development, biotic interactions, and abiotic stress responses in different plant species and have received considerable attention in Arabidopsis and solanaceous species (Suzuki et al. 2011; Torres and Dangl 2005). The NADPH oxidase-dependent oxidative burst was first described as a homologous system to the mammalian superoxide-generating NADPH oxidase of phagocytes, gp91<sup>phox</sup>. Their role in plant interactions with a wide range of pathogens

and symbionts has been extensively documented (Marino et al., 2012). Plant NADPH oxidases, also known as respiratory burst oxidase homologs (RBOHs), are a family of plasma membrane-localized enzymes with homology to the NADPH oxidase from mammalian phagocytes (Torres and Dangl, 2005; Sumimoto, 2008). These enzymes generate apoplastic superoxide ions ( $O_2^{\cdot -}$ ) that rapidly dismutate to hydrogen peroxide ( $H_2O_2$ ) in aqueous solution, either spontaneously or via superoxide dismutase activity. The model plant *A. thaliana* presents a multigene family of 10 Rboh genes (Torres and Dangl, 2005).

Proteomic data showed induced phosphorylation sites in *RBOHD* in Arabidopsis cell cultures treated with the bacterial MAMP Flg22 (Nühse et al. 2007). In addition, application of the calcium ionophore ionomycin and protein phosphatase inhibitor caliculin A suggested that  $Ca^{2+}$  binding and phosphorylation synergistically activates the superoxide-generating enzyme activity of RBOHD (Ogasawara et al. 2008). However, it has recently been described that protein phosphorylation precedes  $Ca^{2+}$  binding in this process (Kimura et al. 2012). Another activation mechanism is the interaction with plant Rac2 homologues, which may act as positive or negative regulators (Torres et al. 2006).

Transgenic Arabidopsis plants knocked down for the RBOHD and RBOHF full-length transcripts demonstrated that both are required for a full oxidative burst during incompatible interactions with the host plant and *P. syringae* pv. *tomato* DC3000 (avrRpm1) or the oomycete parasite *Peronospora parasitica*. The RBOH mutant plants were transposon insertion lines that did not exhibit any normal full-length transcript,

but instead only showed some aberrant transcripts that would presumably give rise to non-functional proteins (Torres et al. 2002). Furthermore, both *rbohD* and *rbohF* knockdown lines are modestly more susceptible to *P. syringae* pv. *tomato* DC3000 (Chaouch et al. 2012; Daudi et al. 2012). There is also evidence that plant NADPH oxidases mediate additional plant biotic interactions, such as the establishment of symbiotic nodules in *Medicago trunculata* (Marino et al. 2011). Triple mutants have been generated by crossing the *rbohD* and *rbohF* mutants with the *lsd1* (lesions simulating disease) mutant, which cannot control the extent of the normal HR, leading to runaway cell death (Torres and Dangl 2005). Thus, it was proposed that RBOH proteins have an antagonistic role to salicylic acid in the HR by limiting the spread of cell death in the tissue surrounding the site of infection.

#### **1.4 Apoplastic class III peroxidase**

There are many different kinds of peroxidases that have been characterized in several different organisms, and the class III peroxidases (EC 1.11.1.7) comprise a small subset of these. Class III peroxidases are widely distributed in the plant kingdom, and have been reported in Chlorophyta, Euglenophyta, Rhodophyta, Byophyta, Pteridophyta, and all the Spermatophyta studied so far (Passardi et al., 2007). They are members of a large multigenic family, with 138 members in rice (Passardi et al., 2004a) and 73 members in Arabidopsis (Welinder et al., 2002). Class III peroxidases are involved in redox reactions, in which H<sub>2</sub>O<sub>2</sub> and other hydroperoxides are typically used as a substrate. However, these enzymes can also generate H<sub>2</sub>O<sub>2</sub> under specific

conditions and the provision of a strong reductant (Berglund et al. 2002; Dunford 1993; Wojtaszek 1997). The peroxidase cycle, in which H<sub>2</sub>O<sub>2</sub> is scavenged, starts with the ferric enzyme, which is in its ground state. The transfer of an oxygen atom from H<sub>2</sub>O<sub>2</sub> to the heme group forms compound I. After one electron addition from a reducing substrate compound II is formed. The cycle finishes after the formation of the ferric enzyme. However, under the presence of a sufficiently potent reductant agent, the ferric enzyme can be reduced to form the ferrous enzyme, which will react with O<sub>2</sub> to form compound III. In addition, this compound can be formed by the reaction of H<sub>2</sub>O<sub>2</sub> with compound II. However, this reaction is unlikely to occur under physiological conditions. Finally, the ferric enzyme is formed by reacting with a proton donor, resulting in H<sub>2</sub>O<sub>2</sub> production.

The apoplastic peroxidase-dependent oxidative burst was first proposed by Bach and co-workers (Bach et al. 1993) who showed that the apoplast, which is the free, diffusional space outside the plasma membrane and within the boundaries of plant cell walls, is required for a full oxidative burst in carrot cultured cells. Several subsequent experiments have shown this mechanism to be operational in *Phaseolus vulgaris* (French bean) (Bolwell et al. 1999, 1995, 2001), *Arabidopsis* (Bindschedler et al. 2006; Daudi et al. 2012; Davies et al. 2006; O'Brien et al. 2012), *Capsicum annum* (Choi et al. 2007), *Lactuca sativa* (Bestwick et al. 1998) and *Gossypium hirsutum* (Martinez et al. 1998).

Among the proteins induced during plant defence and playing a key role in several metabolic responses, class III plant peroxidases are well known. Investigations

in Arabidopsis plants transformed with the antisense sequence of *FBP1* showed reduced levels of H<sub>2</sub>O<sub>2</sub> production when challenged with a fungal extract. In addition, increased susceptibility against a variety of pathogens was found in these transgenic lines (Bindschedler et al. 2006). Measurements of mRNA expression demonstrated that the Arabidopsis class III peroxidases *At3g49110* (*AtPrx33*) and *At3g49120* (*AtPrx34*) were downregulated in these plants. Recently, the role of both *PRX33* and *PRX34* in the oxidative burst and pattern-triggered immunity (PTI) has been further dissected (Daudi et al. 2012; O'Brien et al. 2012). The data from these reports suggests that peroxidase-derived H<sub>2</sub>O<sub>2</sub> production is the main source of ROS during the oxidative burst, but is complemented by additional sources, such as the NADPH oxidase-derived production of ROS. Mature leaves of T-DNA insertion lines with reduced expression of *PRX33* and *PRX34* exhibited low amounts of ROS and callose deposition in response to the MAMPs Flg22 and Elf26, which correspond to bacterial flagellin and elongation factor Tu, respectively. *PRX33* and *PRX34* knockdown lines also exhibited diminished activation of Flg22-activated genes following Flg22 treatment. Proteomic analysis showed that knockdown of *PRX33* and *PRX34* led to the depletion of various MAMP-elicited defence-related proteins including the two cysteine-rich peptides PDF2.2 and PDF2.3 (O'Brien et al. 2012). These MAMP-activated genes were also downregulated in unchallenged leaves of the peroxidase knockdown lines, suggesting that a low level of apoplastic ROS production may be required to pre-prime basal resistance. The *PRX33* knockdown line was also shown to be more susceptible to *Pseudomonas syringae* than wild-type plants. Taken together, these data demonstrate that the

peroxidase-dependent oxidative burst plays an important role in Arabidopsis basal resistance or PTI mediated by MAMP recognition (Daudi et al. 2012). The peroxidase-dependent oxidative burst is not unique to Arabidopsis and French bean, and is also found in other species such as pepper, in which the extracellular peroxidase CaPO2 plays a significant role in generating H<sub>2</sub>O<sub>2</sub> in response to *Xanthomonas campestris* pv. *vesicatoria* (Choi et al. 2007).

## 1.5 Purposes of the study

From the above, among the subsets of the Arabidopsis class III peroxidases family are upregulated by pathogens, salicylic acid (SA), jasmonic acid and ethylene (Almagro et al. 2009), but the precise role still poorly understood for each isoform, due to high complexity for genetic analysis (Oliva et al. 2009; Welinder et al. 2002). Moreover, although it is clear from the data presented in Daudi et al. (2012) and in Bindschedler et al. (2006) that *PRX33* and *PRX34* play important roles in Arabidopsis PTI responses, but the respective roles of *PRX33* and *PRX34* are not completely clear.

In this study, we obtained two additional T-DNA insertion null mutants (referred to as *prx34-2* and *prx34-3*), besides the well-studied *prx34-1*, and characterized these mutants for their responsiveness to bacterial and fungal pathogens. We also generated transgenic Arabidopsis plants overexpressing the *PRX34* to unravel the function of the corresponding peroxidase in disease resistance. Then, to further explore the role of class III peroxidase *PRX34* in plant oxidative burst and immunity.

## **CHAPTER II**

**Some T-DNA Insertion Lines that Affect the Expression of**

***PRX34***

## 2.1. Abstract

We characterized three available Arabidopsis lines homozygous for T-DNA insertions. The insertion of T-DNA and the absence of transcripts were determined by genomic PCR and a reverse transcription and PCR, respectively. Similar to previous observations, *PRX34* expression was not completely abolished in the *prx34-1*, excluding the *prx34-1* for further analyses. In contrast, we could not detect any transcripts in both *prx34-2* and *prx34-3* mutants by quantitative RT-PCR, suggesting loss-of-function mutations. Obviously, a tandem-located *PRX33* expression was not affected in these mutants. In parallel, we also obtained NaCl-solubilized cell wall proteins from individual plants and analyzed accumulation of corresponding peroxidase with an anti-horseradish peroxidase (HRP) antibody. In contrast to considerable accumulation in the wild-type, no or negligible accumulation of proteins was detectable in *prx34-2* and *prx34-3*. Together with the analysis of transcripts, this result indicates that PRX34 is one of the major peroxidases that constitutively accumulate in the mature leaves of Arabidopsis plants. The *prx34-2* and *prx34-3* presented similar phenotypes to the wild-type, indicating no fatal defect in the reproductive growth.

## 2.2 Introduction

Since many plant scientists use Arabidopsis as a model plant for mutational experiments, extensive collections of lines of mutants, as well as comprehensive genetic maps based on biochemical and morphological mutations and on polymorphic DNA markers, are now available. However, one of the best methods for generating the tagged

mutants is based on insertional mutagenesis with the T-DNA from *Agrobacterium tumefaciens* (e.g. Feldmann, 1991; Radhamony et al., 2005). A T-DNA insertion may reveal gene function via a gene knock-out and a gene knock-up (over-expression and miss-expression) or through expression patterns revealed by modified insertion elements. The T-DNA tag typically causes a loss of gene expression and results in a monogenic recessive mutation in the gene.

To generate T-DNA insertion mutants, T-DNA must be inserted randomly in the genome through transformation mediated by *Agrobacterium tumefaciens*. During generation of a T-DNA insertion mutant, *Agrobacterium* competent cells are first prepared and plasmids containing the T-DNA introduced into *Agrobacterium* cells. *Agrobacterium* containing T-DNA vectors are then used to transform T-DNA into *Arabidopsis*. After screening and identifying T-DNA insertion mutants with interesting phenotypes, genomic DNA is extracted from the mutants and used to isolate the T-DNA flanking sequences.

The identification of knockout mutants is the first step toward describing the function of a gene. After the isolation of a mutant line, plants homozygous for the mutation must be identified, outcrossed, and analyzed to ensure that only one T-DNA insertion is present. With a confirmed mutant in hand, the next step is to determine the consequences of the mutation on growth and development relative to the wild type. However, it has become apparent that many knockout mutants have no readily identifiable phenotype. For example, of the 17 mutants described in Krysan et al. (1996), none displays an altered phenotype unless grown under specific conditions (Hirsch et

al., 1998; P.J. Krysan, J.C. Young, and M.R. Sussman, unpublished results). Functional redundancy among the members of a gene family is a likely reason for the frequently observed lack of an identifiable phenotype associated with knockout mutations (Hua and Meyerowitz, 1998). One can easily determine the precise genotype of large numbers of individual plants by using the T-DNA insertion as a PCR marker for the mutant locus.

Because of the large size of the type III peroxidase gene family in *Arabidopsis* (at least 73 type III members), which complicates genetic analysis, and presumed functional redundancy precluded a systematic study of *Arabidopsis* peroxidase mutants, the precise role still poorly understood for each isoform (Oliva et al. 2009; Welinder et al. 2002). Under such circumstances, Bindschedler et al. (2006) constructed transgenic *Arabidopsis* plants expressing an antisense cDNA encoding a French bean class III peroxidase (*FBPI*) to identify key peroxidases involved in ROS generation in *Arabidopsis*. The antisense expression of a heterologous *FBPI* cDNA in *Arabidopsis thaliana* exhibited diminished expression of at least two *PRX33* and *PRX34*, accompanied with the attenuated oxidative burst in response to a fungal elicitor, leading to enhanced susceptibility to a range of fungal and bacterial pathogens (Bindschedler et al. 2006). Further investigation of this knockdown line as well as the *prx33-1* and *prx34-1* T-DNA insertion mutants demonstrated that all of these lines are partially impaired in pattern-triggered immunity (PTI), resulting in enhanced susceptibility to fungal and bacterial pathogens (Bindschedler et al. 2006; Daudi et al. 2012). However, the *prx34-1* (ecotype Col-0) containing the T-DNA insertion in the promotor region of

*PRX34* gene is likely hypomorphic mutant (Arnaud et al. 2017; Passardi et al., 2006).

In this chapter, we characterized three available *Arabidopsis* lines homozygous for T-DNA insertions. Besides the well-studied *prx34-1*, we obtained two additional *Arabidopsis prx34* null mutants (*prx34-2*, *prx34-3*) to investigate the role of class III peroxidase PRX34 in oxidative burst and immunity in *Arabidopsis*.

## 2.3 Materials and Methods

### 2.3.1 Plant Materials and Growth Conditions

*Arabidopsis (Arabidopsis thaliana)* mutant lines in the Col-0 background. The *prx34-1* (SALK\_051769) and *prx34-2* (GK-728F08) were purchased from the Salk T-DNA insertion line (Alonso et al. 2003) and the Nottingham *Arabidopsis* Stock Centre, respectively. Homozygous T-DNA insertion mutants in *PRX34* (*prx34-1* and *prx34-2*) were selected by PCR with loci-specific primers in combination with T-DNA border 100 primer (BP) (Fig. 2.1; Fig. 2.2). A homozygous *prx34-3* (SALK\_112466C) was also obtained from the Salk T-DNA insertion line (Fig. 2.1; Fig. 2.2). All T-DNA insertion mutants were confirmed by genotyping prior to usage using PCR primers (Table 2.1). Seeds were sown on a 1:1 mixture of vermiculite:peat (Supermix-A soil; Sakata Seed Co.,Ltd., Yokohama, Japan) and grown in a chamber at 22°C, with a 10 h light/14 h dark cycle at 11.8 W m<sup>-2</sup>.

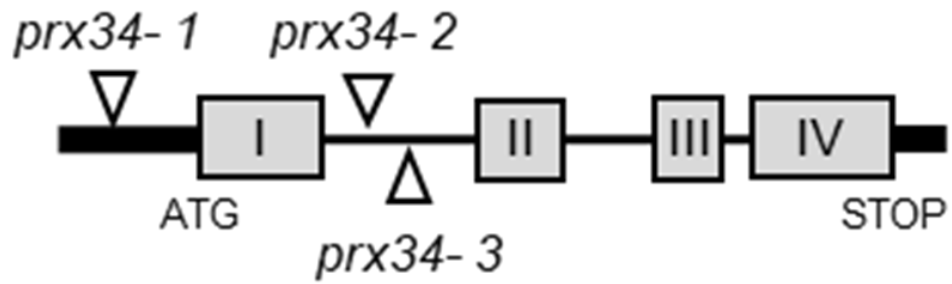


**Figure 2.1** Gene organization of *AtPRX34* (*At3g49120*) and insertion sites of T-DNA. Grey boxes represent exons (numbered from I to IV) and black lines introns. Bold lines are the predicted 5' and 3' UTR. The arrows indicated a primer set used for transcript analysis.

**Table 2.1** Summary information for primer sequences used to genotype *prx34* mutants

<b>Genotype</b>	<b>Mutation</b>	<b>Primer name</b>	<b>Sequence (5' &gt; 3')</b>	<b>Primer site</b>
<i>prx34-1</i>	SALK_051769	Salk_LBb1	GCGTGGACCGCTTGCTGCAACT	Left T-DNA border primer
		LP	TATTTTCGTGAATCCGATTGC	Left genomic primer
		RP	TCCGTTAGCGTTCCACATTAG	Right genomic primer
<i>prx34-2</i>	GK-728F08	GABI_LB_o8409	ATATTGACCATCATACTCATTGC	Left T-DNA border primer
		LP	CTTCCATGTAGATAGCGTGG	Left genomic primer
		RP	TGCCATTCACTAAAACCATTTG	Right genomic primer
<i>prx34-3</i>	SALK_112466C	Salk_LBb1	GCGTGGACCGCTTGCTGCAACT	Left T-DNA border primer
		LP	CTTCCATGTAGATAGCGTGG	Left genomic primer
		RP	TGCCATTCACTAAAACCATTTG	Right genomic primer

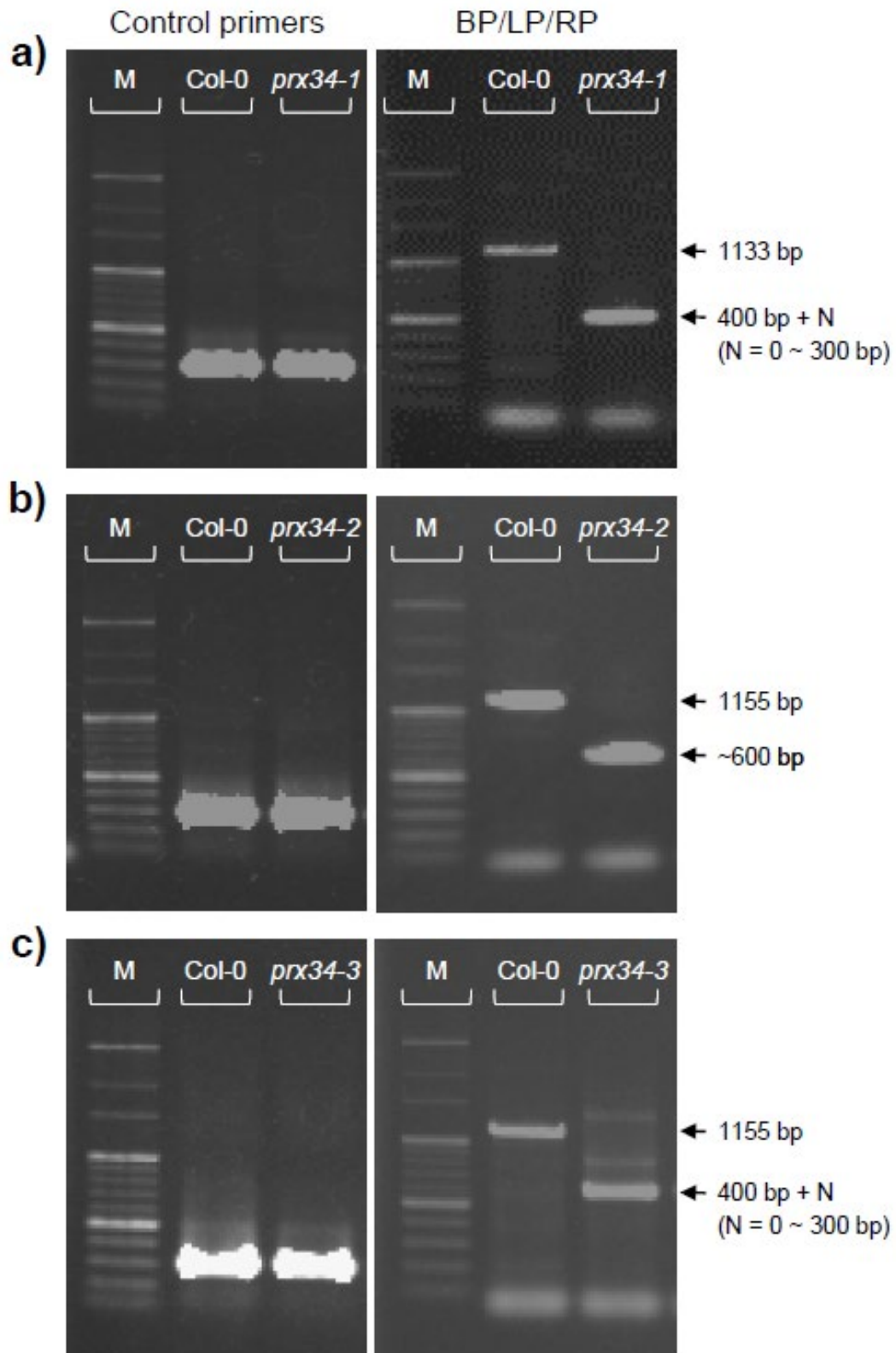


**Figure 2.2** Genotyping for three *prx34* mutants. PCR was performed with a Thermo Scientific Phire Plant Direct PCR Kit (Thermo Scientific) using genomic DNAs of the *prx34-1* (SALK\_051769) (a), *prx34-2* (GABI\_728F08) (b) or *prx34-3* (SALK\_112466C) (c), respectively. Control amplification was carried out with primers supplied with the kit that amplifies a 297 bp fragment of a highly conserved region of chloroplast DNA. Wild-type Col-0 was used as the control. The T-DNA border primer (BP), left (LP) and right (RP) genomic primers for each mutant line were designed according to the T-DNA Primer Design (<http://signal.salk.edu/tdnaprimers.2.html>) and were listed in Supplementary Table 1. The RP was always on the side of the flanking sequence (the 3' end of the insertion). Therefore, by using the three primers (BP+LP+RP), the wild-type (no insertion) gave an amplicon of about 1100 bp (from LP to RP). For homozygous insertion lines, the PCR amplified a distinct band of 410 + N bp (from RP to insertion site 300 + N bases, plus 110 bases from BP to the left border of the vector).

### 2.3.2 RNA Extraction and Quantitative RT-PCR Analysis

Leaves were harvested and immediately frozen in liquid nitrogen. One hundred milligrams of material was ground in liquid nitrogen, and total RNA was extracted with the Plant Total RNA purification Kit (GMBiolab) according to the manufacturer's instructions. After quantification by spectrophotometry and confirmation by electrophoresis, 1 µg of the crude RNA preparations was treated with one unit of RNase-free DNase I. The DNA-free RNA was then used as a template for reverse transcription according to the ImProm-II RT protocol. Quantitative (q)PCR was performed with a Shimadzu GVP-9600 Gene Detection System (Shimadzu, Kyoto, Japan), using primer sets listed in Table 2.2.

**Table 2.2** Summary information for primer sequences used to analyze the *PRX33* and

*PRX34* transcripts

Gene	TAIR locus	Forward (5' > 3')	Reverse (5' > 3')
<i>PRX33</i>	At3g49110	TCAATGTCCTCGCAATGGTA	GATTGTGTCAGTGGCATTGG
<i>PRX34</i>	At3g49120	AGTTAAGGTCGGACCCTCGT	GAGCTGCAATGGTGAGCATA
<i>EF1-α</i>	At1g07920	CATCATTGGCACCCCTTCTT	TGGTGACGCTGGTATGGTTA

### 2.3.4 Cell Wall Proteins Extraction

NaCl-solubilized cell wall proteins from individual plants as described previously Verdonk et al. (2012). Briefly, the Arabidopsis leaves was placed in a 50 ml Falcon® tube with 20 mL of buffer A (5 mM Na acetate, 0.4 M sucrose, pH 4.6, 4°C), shaken vigorously (24 Hz, 2 min) and placed on a rocking platform (overnight, 4°C). Samples were then centrifuged (1000 g, 15 min, 4°C) and supernatants were discarded. Both pellets were resuspended in 10 mL of buffer B (5 mM Na acetate, 0.6 M sucrose, pH 4.6, 4°C) and placed on a rocking platform (30 min, 4°C) and centrifuged again (1000 g, 15 min, 4°C). Supernatants were discarded. This washing step was repeated respectively with buffer C (5 mM Na acetate, 1 M sucrose, pH 4.6, 4°C) and twice with buffer D (5 mM Na acetate, pH 4.6, 4°C). The isolated cell wall fractions (pellet) were then transferred to 30 mL tubes.

The proteins from the isolated cell wall fraction (pellet) were extracted with 7.5 mL of extraction buffer 5 (5 mM Na acetate, 200 mM CaCl<sub>2</sub>, pH 4.6, 4°C) and placed on a rocking platform (30 min, 4°C). Samples were then centrifuged (10,000 g, 15 min, 4°C) and supernatants saved. This step was repeated once and supernatants were pooled, leading to the CaCl<sub>2</sub> fraction.

Proteins were further extracted with 10 mL of extraction buffer 3 (5 mM Na acetate, 50 mM EGTA, pH 4.6) and shaken vigorously at 37°C for 1 h. After centrifugation (10,000 g, 15 min, 4°C), supernatants were saved. This extraction step was repeated twice and supernatants were pooled leading to the EGTA fraction.

The remaining pellet was finally resuspended in 15 mL of extraction buffer 4 (5

mM Na acetate, 3 M LiCl, pH 4.6, 4°C), placed on a rocking platform (overnight, 4°C) and centrifuged (10,000 g, 15 min, 4°C). Supernatants were saved, forming the LiCl fraction.

### **2.3.5 Detection of PRX34 Corresponding Peroxidase by Immunoblotting**

Equal amounts of cell wall proteins (1.5 µg) were separated with SDS-PAGE and transferred onto a PVDF membranes. The membrane was probed with an anti-horseradish peroxidase (HRP) antibody (1:10,000) (GTX22110; GeneTex, Irvine, CA, USA).

### **2.3.6 Statistical Analysis**

All results are expressed as mean ± standard deviation (SD). Statistical evaluations were performed using Graph-pad Prism version 7 (GraphPad Software, Inc., San Diego, CA, USA). The data were subjected to analysis of one-way ANOVA, followed by Dunnett's multiple comparison test. Differences at  $P \leq 0.05$  were considered significant.

## **2.4 Results**

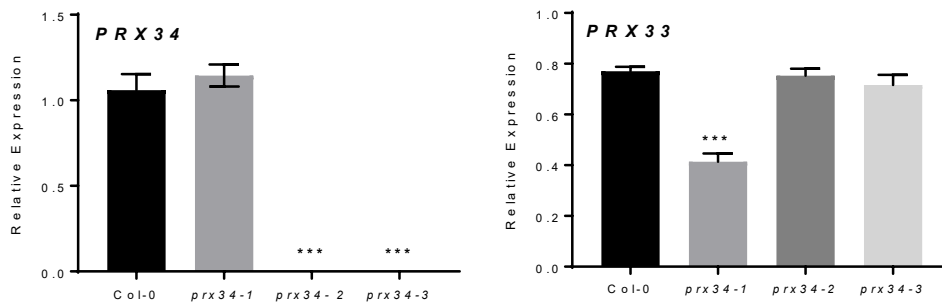
### **2.4.1 Identification of *prx34* T-DNA mutants**

To analyze the function of PRX34 peroxidase in plant oxidative burst and immunity, we isolated three available Arabidopsis lines homozygous for T-DNA insertions (*prx34-1*, *prx34-2* and *prx34-3*). All lines harbor a T-DNA located in the promoter region and intron (Fig. 2.1), respectively. Similar to previous observations

(Daudi et al. 2012; Lyons et al. 2015; Passardi et al. 2006), *PRX34* expression was not completely abolished in the *prx34-1* (Fig. 2.3a), excluding the *prx34-1* for further analyses. In contrast, we could not detect transcripts in both *prx34-2* and *prx34-3* mutants by quantitative RT-PCR (Fig. 2.3a), suggesting loss-of-function mutations. *PRX33* and *PRX34*, which are contiguous genes, show nearly 95% homology at the protein level, but their promoter and intronic sequences are highly divergent (Vale' rio et al., 2004). To determine more precisely whether the expression of *PRX33* is affected or not, quantitative RT-PCR analyses was performed on leaves of 4-week-old wild-type and three *prx34* mutant lines. Obviously, *PRX33* expression was not affected in these mutants.

Detailed phenotypic characterization was carried out on these three transgenic lines. The *prx34-2* and *prx34-3* are similar germination and vegetative growth to the wild-type, indicating no fatal defect in the reproductive growth (Fig. 2.3b).

**a)**



**b)**



**Figure 2.3** Phenotypic and molecular characterization of *atprx34* mutants. **(a)** *PRX34* transcript levels in 4-week-old seedlings of the wild-type, *prx34-1*, *prx34-2* and *prx34-3*. A quantitative RT-PCR was performed with a Shimadzu GVP-9600 Gene Detection System (Shimadzu, Kyoto, Japan), using primer sets listed in Table 2. The expression level was normalized by the *EF1- $\alpha$*  gene (*At1g07920*). *PRX33* were quantified similarly. The expression level of each gene was normalized by the *EF1- $\alpha$*  (*At1g07920*) gene. Data are shown as the average  $\pm$  standard deviation (SD) from three independent plants. Asterisk indicate significant difference (Dunnett's test; \*\*\*,  $p < 0.001$ ). **(b)** Growth of 4-week-old seedlings.

#### 2.4.2 *prx34-2* and *pr34x-3* mutations impaired in accumulation of corresponding peroxidase

In parallel, we also obtained NaCl-solubilized cell wall proteins from individual plants as described previously (Kiba et al. 1997; Toyoda et al. 2012), and analyzed accumulation of corresponding peroxidase with an anti-horseradish peroxidase (HRP) antibody (Fig. 2.4a). In contrast to considerable accumulation in the wild-type, no or negligible accumulation of proteins was detectable in *prx34-2* and *prx34-3*, but not in *prx34-1* (Fig. 2.4a).

In order to examine the role of PRX34 in the ROS generation, NaCl-solubilized cell wall proteins from the wild-type, *prx34-2* and *prx34-3* were tested for their ROS generating activity. Remarkably, the ROS-generation requiring manganese ion ( $Mn^{2+}$ ), *p*-coumaric acid (*p*-CA) and NADH as an electron donor was significantly less in the extracts of *prx34-2* and *prx34-3*, likely due to decrease in the corresponding peroxidases (Fig. 2.4b). Together with the analysis of transcripts (Fig. 2.3a), this result indicates that PRX34 is one of the major peroxidases that constitutively accumulate in the mature leaves of Arabidopsis plants.

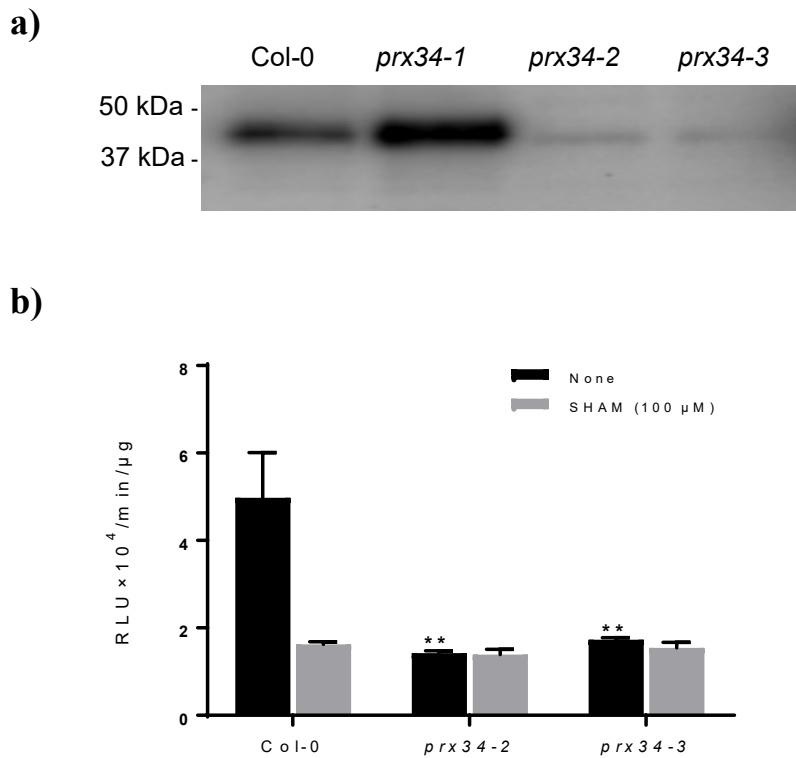


**Figure 2.4** Reduced ROS generation and decreased peroxidase activity in *prx34-2* and *prx34-3* mutants. **(a)** Western blot analysis of peroxidase accumulation in 4-week-old seedlings of the wild-type and *prx34* mutants. NaCl-solubilized cell wall proteins were obtained according to the method described previously (Kiba et al. 1997; Toyoda et al. 2012). Equal amounts of cell wall proteins (1.5  $\mu$ g) were separated with SDS-PAGE and transferred onto a PVDF membranes. The membrane was probed with an anti-horseradish peroxidase (HRP) antibody (1:10,000) (GeneTex, Irvine, CA, USA). **(b)** Generation of ROS in cell wall extracts through NADH oxidation. The cell wall proteins (0.25  $\mu$ g) from individual plants were incubated in a reaction mixture (50  $\mu$ l) containing 30 mM Tris/MES (pH 6.5), 0.5 mM NADH, 0.5 mM *p*-coumaric acid (*p*-CA) and 20 mM  $\text{MnCl}_2$  and 10  $\mu$ M MPEC (ATTO Co.,Ltd., Tokyo, Japan) without or with 100  $\mu$ M of salicylhydroxamic acid (SHAM). Chemiluminescence (RLU) was measured with a

Lumat LB9507 (Berthold Technologies, Bad Wildbad, Germany) for 2 min. Data represent the average  $\pm$  SD of three replicates. Asterisks indicate significant difference (Dunnett's test; \*\*\*,  $p < 0.001$ ).

## 2.5 Discussion

Bindschedler et al. (2006) constructed transgenic Arabidopsis plants expressing an antisense cDNA encoding a French bean class III peroxidase (FBP1) to identify key peroxidases involved in ROS generation in Arabidopsis. The antisense expression of a heterologous FBP1 cDNA in Arabidopsis thaliana exhibited diminished expression of at least two *PRX33* and *PRX34*, accompanied with the attenuated oxidative burst in response to a fungal elicitor, leading to enhanced susceptibility to a range of fungal and bacterial pathogens (Bindschedler et al. 2006).

Because the *prx34-1* (ecotype Col-0) containing the T-DNA insertion in the promoter region of *PRX34* gene in previous work (Bindschedler et al. 2006; Daudi et al. 2012) is likely hypomorphic mutant (Arnauld et al. 2017; Passardi et al., 2006). Indeed, we could detect transcripts from mature leaves of *prx34-1* by PCR with reverse transcription (RT-PCR) (see Fig. 2.3a), suggesting that the expression of *PRX34* was not severely abolished in the *prx34-1*. In addition, the tandem-duplicated *PRX33* gene in the *prx34-1* was unwantedly affected under our laboratory conditions.

Gross et al. (1977) and Halliwell (1978) reported, using cell wall-bound peroxidases or purified horseradish peroxidases, the oxidation of NADH leads to the generation of  $O_2^-/H_2O_2$  through a complex pathway involving apoplastic NADH, NAD

and NAD<sup>+</sup>. Halliwell (1978) also demonstrated that peroxidase-catalyzed H<sub>2</sub>O<sub>2</sub>/O<sub>2</sub><sup>-</sup> generation largely depends on both Mn<sup>2+</sup> and phenolic compounds such as *p*-CA. In fact, exclusion of either NADH, Mn<sup>2+</sup> or *p*-CA significantly lowered the O<sub>2</sub><sup>-</sup>-generating activity in extracts from Arabidopsis cell walls, confirming that cell wall peroxidase(s) itself is capable of generating ROS through the oxygen-requiring cycle independently of H<sub>2</sub>O<sub>2</sub> as reported previously (Kimura and Kawano 2015). Collectively, PRX34 is likely one of the important isoforms that generate ROS through the oxidation of NADH.

# **Chapter III**

## **Peroxidase Knockout Lines are Compromised in Flg22- Elicited Immune Responses**

### **3.1 Abstract**

We investigated whether PRX34 contributes to disease resistance in *Arabidopsis*. Infection assay with *prx34* mutants was performed using virulent strains of fungal and bacterial pathogens such as *Botrytis cinerea*, *Colletotrichum higginsianum* and *Pectobacterium carotovorum* subsp. *carotovorum*. Interestingly, regardless of pathogens tested, the drop inoculation assays clearly showed that, compared to the wild-type, lesion area significantly increased on *prx34-2* and *prx34-3*. Consistent with this result, these mutants reduced typical PTI responses such as accumulation both of ROS and callose when exposed to Flg22 peptide as a bacterial MAMP. These results indicated that PRX34 is a component of PTI and that is necessary for full resistance to virulent pathogens.

### **3.2 Introduction**

#### **3.2.1 *Botrytis cinerea***

The pathogen *Botrytis cinerea* Pers. Fr. (teleomorph *Botryotinia fuckeliana* (de Bary) Whetzel) causes serious losses in more than 200 crop species worldwide. It is most destructive on mature or senescent tissues of dicotyledonous hosts, but it usually gains entry to such tissues at a much earlier stage in crop development and remains quiescent for a considerable period before rapidly rotting tissues when the environment is conducive and the host physiology changes. Therefore, serious damage is caused following harvest of apparently healthy crops and the subsequent transport to distant markets where the losses become evident. However, *B. cinerea* also causes massive

losses in some field- and greenhouse-grown horticultural crops prior to harvest, or even at the seedling stage in some hosts. *B. cinerea* is responsible for a very wide range of symptoms and these cannot easily be generalized across plant organs and tissues. Soft rots, accompanied by collapse and water-soaking of parenchyma tissues, followed by a rapid appearance of grey masses of conidia are perhaps the most typical symptoms on leaves and soft fruits. Droby and Lichter (2004) provide a comprehensive list of post-harvest rots caused by *B. cinerea*; these range from grey mould on different plant organs, including flowers, fruits, leaves, shoots and soil storage organs (i.e. carrot, sweet potato), although the fungus is not regarded as a true root pathogen or one causing soil-borne diseases. Vegetables (i.e. cabbage, lettuce, broccoli, beans) and small fruit crops (grape, strawberry, raspberry, blackberry) are most severely affected. It has become an important model for molecular study of necrotrophic fungi.

### **3.2.2 *Pectobacterium carotovorum***

*Pectobacterium carotovorum* subsp. *carotovorum* (formerly *Erwinia carotovora* subsp. *carotovora*) is a Gram-negative phytopathogen responsible for soft rot disease, wilt, or blackleg in various crops, by producing plant cell wall degrading enzymes that are actively secreted by the bacterium. Several important crops, such as Chinese cabbage and potato, have been attacked by this pathogen, and large economic losses resulting from significant yield reductions in the field, in transit, and during storage have occurred (Gardan et al. 2003, Marquez et al. 2011, Ravensdalea et al. 2007, Whitehead et al. 2002).

The main symptoms caused by *Pectobacterium carotovorum* include wilting and water-soaked lesions, which may lead to stem collapse. Soft rot symptoms may include browning of stem and pith in tomatoes, especially when ripe fruit is infected. Changes develop quickly after stem collapse, such as skin folding and cracking followed by development of creamy white ooze (Blancard et al. 1994). Water-soaked lesions may develop on the outside of fruits and vegetables. Over time, these lesions will sink and may form pits as the bacteria rots away the middle lamella (Bartz 1991).

### **3.2.3 *Colletotrichum higginsianum***

*Colletotrichum* is a large ascomycete genus comprising more than 190 species, many of which cause devastating diseases on a large range of agricultural and horticultural crops worldwide (Jayawardena et al. 2016). Among species of *Colletotrichum*, *C. higginsianum* is classified in a main phylogenetic clade within the *C. destructivum* complex, and causes anthracnose disease on a wide range of cruciferous plants, such as species of *Brassica* and *Raphanus* as well as the model plant *Arabidopsis thaliana* (Damm et al. 2014, Crouch et al. 2014, Narusaka et al. 2006). Since most *A. thaliana* ecotypes are susceptible to *C. higginsianum*, the pathogen can be regarded as adapted for *A. thaliana* (Shimada et al. 2006).

As a typical hemibiotrophic fungus, *C. higginsianum* develops a series of specialized infection structures including germ tubes, appressoria, primary biotrophic hyphae (BH), and secondary necrotrophic hyphae (NH).

At the start of the hemibiotrophic life cycle of *C. higginsianum* on *Arabidopsis*,

conidia land on the leaf surface and produce germ tubes, which then produce appressoria to penetrate the leaf surface (De Silva et al. 2017). As they mature, cell walls of appressoria become melanized while suitable solutes will accumulate in the cytoplasm. High turgor pressure builds up by water diffusion into appressoria, which provides the force for the peg to penetrate through the plant cell wall. Within a breached epidermal cell, the initial narrow hypha from the peg gives rise to a swollen, sac-like BH. The BH enlarge and form lateral bulbous lobes, resembling a haustorium. The fungus establishes itself as a biotroph within 36 h post infection by forming a multiseptate, multilobed structure, variable in shape and confined within the initially infected epidermal cells. At this stage of the interaction, infected cells can still plasmolyse normally, and the host plasmalemma and tonoplast remained functional (Latunde et al. 1996). Upon subsequent colonization of neighbouring cells at 72 h post-infection, a switch in both hyphal morphology and trophic relationship occur. At the periphery of the lobed BH, outgrowths develop rapidly to produce narrow NH. These numerous hyphae radiating from each BH grow through the adjacent cell walls and infect surrounding cells. Narrow NH grow rapidly, and hyphal spread will eventually lead to necrotic lesions with the appearance of water-soaked lesions on the surface of the infected host as soon as 84 h post-infection (Münch et al. 2008). In necrotic tissues, acervuli form to produce numerous conidia.

### **3.2.4 Callose**

Callose-containing cell-wall appositions, called papillae, are effective barriers

that are induced at the sites of attack during the relatively early stages of pathogen invasion. Callose is an amorphous, high-molecular weight  $\beta$ -(1,3)-glucan polymer that serves as a matrix in which antimicrobial compounds can be deposited, thereby providing focused delivery of chemical defenses at the cellular sites of attack. Callose deposition is typically triggered by conserved PAMPs. (Brown et al. 1998; Gomez-Gomez et al. 1999a). Examples of bacterial PAMPs are the 22-amino acid sequence of the conserved N-terminal part of flagellin (Flg22) (Gomez-Gomez and Boller 2000) and the bacterial elongation factor EF-Tu (Elf18) (Kunze et al. 2004). Chitin, a  $\beta$ -(1,4)-linked polymer of N-acetylglucosamine, and chitosan, a randomly distributed  $\beta$ -(1,4)-linked polymer of D-glucosamide and acetylglucosamine, are examples of potent callose-inducing PAMPs from fungal cell walls (Iritri and Faoro 2009). Apart from PAMPs, endogenous elicitors from pathogen- or herbivore-damaged plant tissues can activate callose depositions as well. Well-known examples of damage-associated patterns (DAMP) are oligogalacturonides (OG) (Ridley et al. 2001).

Activity of the downstream pathways is marked by common signaling events, such as anion fluxes, protein phosphorylation cascades, accumulation of ROS, and defense gene induction (Boller and Felix 2009; Jeworutzki et al. 2010; Nicaise et al. 2009). Recently, PAMP or DAMP-induced callose deposition in cotyledons or leaves of *Arabidopsis* has emerged as a popular marker response to study the signaling pathways controlling PTI or the suppression of these pathways by virulence-promoting pathogen effectors. The advantage of this model system is that it allows for rapid and relatively simple screening of PTI activity. The model system has been used to

demonstrate that ROS act as positive signals in Flg22- and OG-induced callose (Galletti et al. 2008; Zhang et al. 2007)

### **3.3 Materials and Methods**

#### **3.3.1 Plant Materials and Growth Conditions**

Plant Materials and Growth Conditions was described in Chapter 2.

#### **3.3.2 Infection Assays**

*Pectobacterium carotovorum* subsp. *carotovorum* strain Pc1 was cultured overnight in liquid Luria-Bertani (LB) medium at 28°C. The bacteria were pelleted using centrifugation and washed twice with and then resuspended in 10 mM MgSO<sub>4</sub>. The amount of bacteria in the infection suspension was adjusted to  $1 \times 10^5$  cfu/ml. Infection was initiated by wounding the surfaces of 4-week-old plant leaves with a pipette tip syringe and then applying 5 µl of bacterial solution to the wound site. Three leaves were infected per plant, and these three leaves were combined to represent one biological sample. The plants were covered with plastic lids to keep the moisture level high.

*Botrytis cinerea* (MAFF712189) was cultured on potato dextrose t agar (PDA) plates. Spores were harvested in maltose medium and filtered through Miracloth (Calbiochem) to remove hyphae. Droplets of 5 µL spore suspension ( $2 \times 10^5$  conidia/mL) were applied to the leaves of 4-week-old plants for quantification of lesion size (mm) after 72 h. Three fully expanded leaves per plant were infected. The plants were covered

with plastic lids to keep the moisture level high and transferred to growth chamber 180  $\mu\text{mol m}^{-2} \text{s}^{-1}$ , 8 h light/16 h dark at 23°C/18°C (day/night).

The *Colletotrichum higginsianum* (MAFF305635) was cultured on potato dextrose agar (PDA) at 25°C and stored in PDA slants at 4°C for further use. Spores were harvested and filtered through Miracloth (Calbiochem) to remove hyphae. Droplets of 5  $\mu\text{L}$  spore suspension ( $2 \times 10^5$  conidia/mL) were applied to the cut off leaves from 4-week-old plants for quantification of lesion size (mm) after 72 h.

### **3.3.3 Assay for Callose Formation**

In situ detection of callose was performed using aniline blue staining adapted from methods used previously (Jacobs et al., 2003; Clay et al., 2009). Briefly, three rosette leaves from 23- to 25-d-old *Arabidopsis* plants were syringe-infiltrated with ~0.1 mL of a diluted microbial 100 nM Flg22, and placed under high humidity (~85% humidity) for 18 h. At least five independent plants were used as biological replicates, and three rosette leaves were sampled from each plant. The experiment was repeated at least two times. After infiltration and overnight incubation, leaves were harvested and placed in sterile 12-well plates. Acetic acid:ethanol (1:3) was added over 8 h with two changes to destain the chlorophyll from the leaf, followed by ethanol (50% v/v) for 1 h, ethanol (30% v/v) for 1 h, and finally dH<sub>2</sub>O for 2 h with two changes. During the washing steps, the 12-well plates containing the leaves were placed on a constant shaker at 120 rpm to ensure even destaining and rehydration of the leaves. After that, the leaves were stained with 5 mg/mL aniline blue in 150 mM sodium

phosphate (pH 7.0) for at least 30 min in the dark. Leaves were mounted in glycerol (50% v/v) and examined under fluorescence microscopy.

### **3.3.4 Detection of Reactive Oxygen Species**

DAB and NBT staining for hydrogen peroxide and superoxide, respectively. *In situ* detection of hydrogen peroxide was performed by vacuum infiltration with 0.1% DAB (Diaminobenzidine tetrahydrochloride, ) using an adaptation of a previous method (Thordal-Christensen et al., 1997; Bindschedler et al., 2006). Briefly, ~100 mL of a diluted microbial elicitor solution 100 nM Flg22 was infiltrated individually into mature rosette leaves from 28- to 30-d-old Arabidopsis plants using a needleless 1-mL syringe. After 2h, leaves were harvested and infiltrated under gentle vacuum with 1mg/mL DAB containing Tween 20 (0.05% v/v) and 10 mM sodium phosphate buffer (pH 7.0). The staining reaction was terminated 5 h after DAB infiltration, and leaves were fixed in ethanol:glycerol:acetic acid 3:1:1 (bleaching solution) placed in a water bath at 95°C for 15 min. Leaves were reimmersed in bleaching solution until chlorophyll was completely depleted and then were visualized under white light and photograph.

For superoxide staining, infiltrated leaves were vacuum infiltrated for 10 min at 60 KPa pressure with 0.1% NBT (Nitro blue tetrazolium) and then incubate at room temperature for 30min under room light. After incubation, dip the samples in boiling absolute ethanol for 5 min, and then rinsed twice with 50% ethanol and once with MQ water. The leaves include in these experiments were from at least six independent plants.

## 3.4 Results

### 3.4.1 *prx34-2* and *prx34-3* mutant plants exhibit enhanced susceptibility to *B. cinerea*, *C. higginsianum* and *P. carotovorum* subsp. *carotovorum*

We further investigated whether PRX34 contributes to disease resistance in *Arabidopsis*, infection assay with *prx34* mutants was performed using virulent strains of fungal and bacterial pathogens such as *B. cinerea*, *C. higginsianum* and *P. carotovorum* subsp. *carotovorum*. Interestingly, regardless of pathogens tested, the drop inoculation assays clearly showed that, compared to the wild-type, lesion area significantly increased on *prx34-2* and *prx34-3* (Fig. 3.1). In contrast, no enhanced susceptibility phenotype was observed in the *prx34-1* when challenged with virulent pathogens such as *B. cinerea*, *C. higginsianum* and *P. carotovorum* subsp. *carotovorum* (Fig. 3.2).

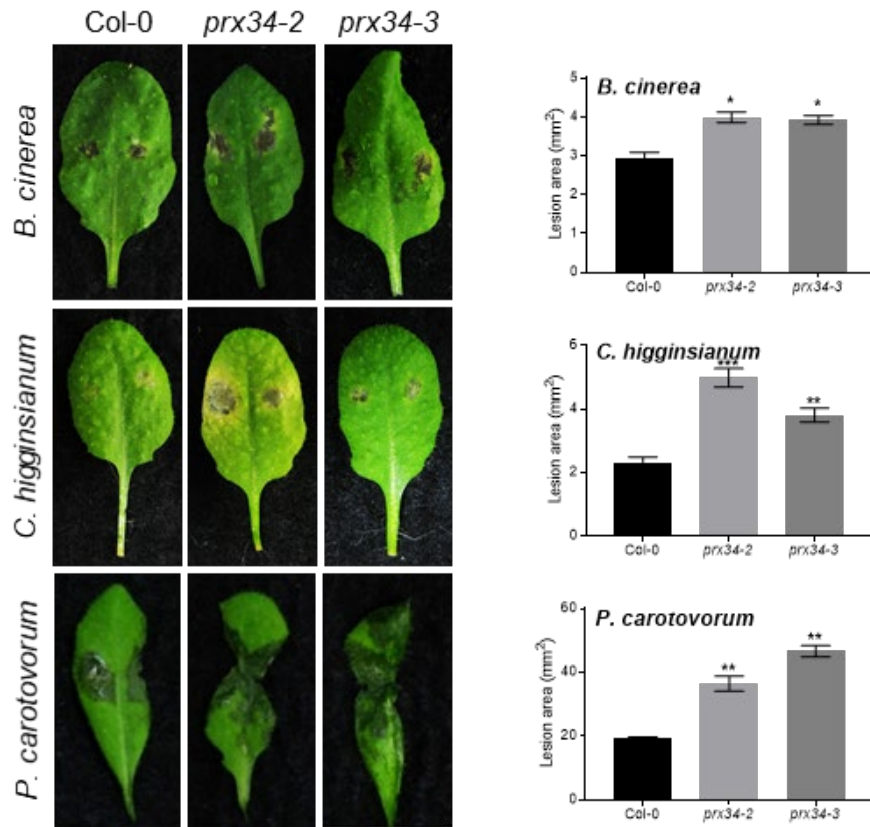


**Fig. 3.1** Enhanced susceptibility of *prx34* mutants to fungal and bacterial pathogens. Disease symptoms induced by *Botrytis cinerea* (MAFF712189), *Colletotrichum higginsianum* (MAFF305635) and *Pectobacterium carotovorum* subsp. *carotovorum* strain Pc1. *B. cinerea* was inoculated by placing 5- $\mu$ l drop of a suspension ( $2 \times 10^5$  conidia/ml) in 1% Sabouraud Maltose Broth onto both side of the middle vein of the detached leaves of 4-week-old wild-type, *prx34-2* and *prx34-3*. *C. higginsianum* ( $2 \times 10^5$  conidia/ml) was inoculated similarly. For inoculation with *P. carotovorum* subsp. *carotovorum* strain Pc1, 5- $\mu$ l drop of a bacterial suspension ( $1 \times 10^5$  cfu/ml) was placed onto injured leaves. All inoculated leaves were incubated for 2 or 3 days at 22°C before taking photos and measuring the lesion size. Data represent the average  $\pm$  SD of ten leaves from 5 independent plants. Asterisks indicate significant difference (Dunnett's test: \*,  $p < 0.05$ ; \*\*,  $p < 0.01$ ; \*\*\*,  $p < 0.001$ ).

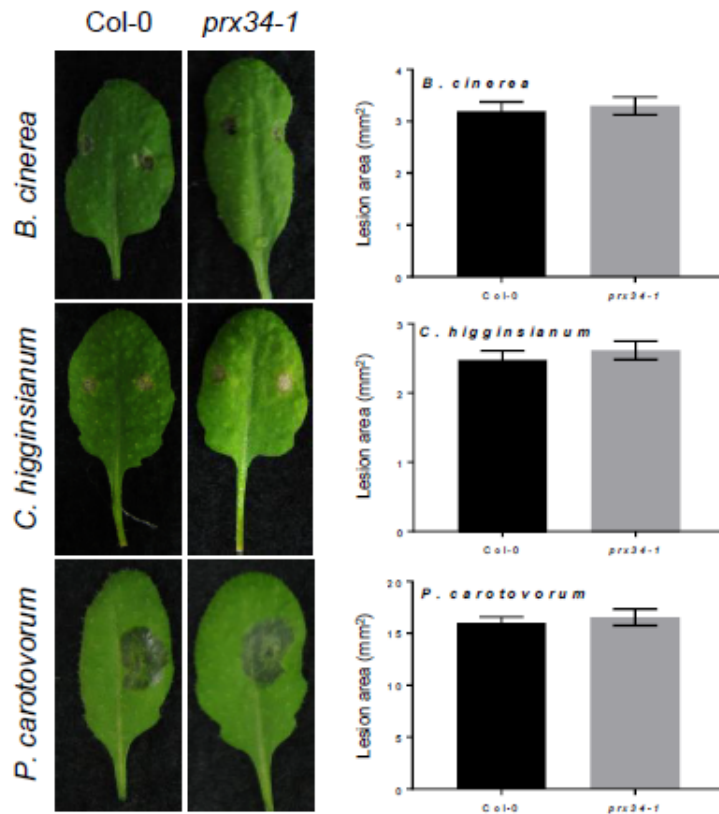


**Fig. 3.2** Response of *prx34-1* mutants to fungal and bacterial pathogens. Disease symptoms induced by *Botrytis cinerea* (MAFF712189), *Colletotrichum higginsianum* (MAFF305635) and *Pectobacterium carotovorum* subsp. *carotovorum* strain Pc1. *B. cinerea* was inoculated by placing 5- $\mu$ l drop of a suspension ( $2 \times 10^5$  conidia/ml) in 1% Sabouraud Maltose Broth onto both side of the middle vein of the detached leaves of 4-week-old wild-type and *prx34-1*. *C. higginsianum* ( $2 \times 10^5$  conidia/ml) was inoculated similarly. For inoculation with *P. carotovorum* subsp. *carotovorum* strain Pc1, 5- $\mu$ l drop of a bacterial suspension ( $1 \times 10^5$  cfu/ml) was placed onto injured leaves. All inoculated leaves were incubated for 2 or 3 days at 22°C before taking photos and measuring the lesion size. Data represent the average  $\pm$  SD of ten leaves from 5 independent plants. Asterisks indicate significant difference (Dunnett's test: \*,  $p < 0.05$ ; \*\*,  $p < 0.01$ ; \*\*\*  $p < 0.001$ ).

### 3.4.2 *prx34-2* and *prx34-3* mutations are compromised in Flg22-elicited immune responses

The absence of *PRX34* transcript and corresponding peroxidases accumulation suggested that the MAMP-mediated responses are affected in *prx34-2* and *prx34-3* mutations. To explore this hypothesis, we treated plants with Flg22 peptide as a bacterial MAMP. Indeed, the *prx34* null mutant resulted in lower levels of superoxide and hydrogen peroxide accumulation in the leaves of the *prx34-2* and *prx34-3* mutant plants than in the wild-type plants (Fig. 3.3a), indicating reduced peroxidase activity. This result in agreement with the observation of an enhanced susceptibility to pathogens. In contrast, *prx32* mutation exhibited the wild-type levels of NBT and DAB staining, respectively (Fig. 3.4a). These results suggest that PRX34 but not PRX32 play an important role in ROS generation in response to Flg22.

In addition to the activation of an oxidative burst, another well-studied MAMP-elicited response in Arabidopsis is the deposition of callose,  $\alpha$   $\beta$ -1,3-glucan polymer that is believed to strengthen and plug weak or compromised sections of plant cell walls. Its deposition at the site of pathogen attack has been extensively studied. As expected, *prx34-2* and *prx34-3* mutant plants exhibited significantly reduced levels of callose deposition in response to the Flg22 (Fig. 3.3b).

Unfortunately, *prx34-1* mutation also exhibit reduced levels of callose deposition in response to the Flg22 (Fig. 3.4b), probably due to unwanted suppression of *PRX33*-mRNA (Fig. 2.3a). It is mean PRX33 may play an additional role in ROS generation in response to flg22.

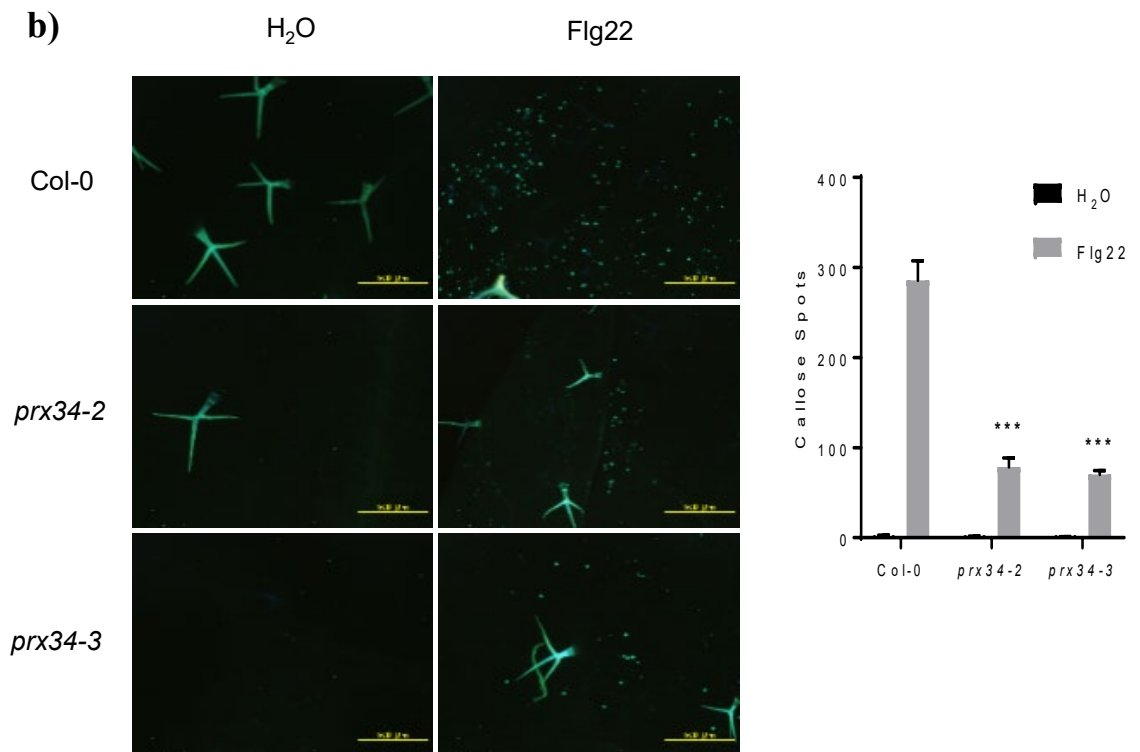
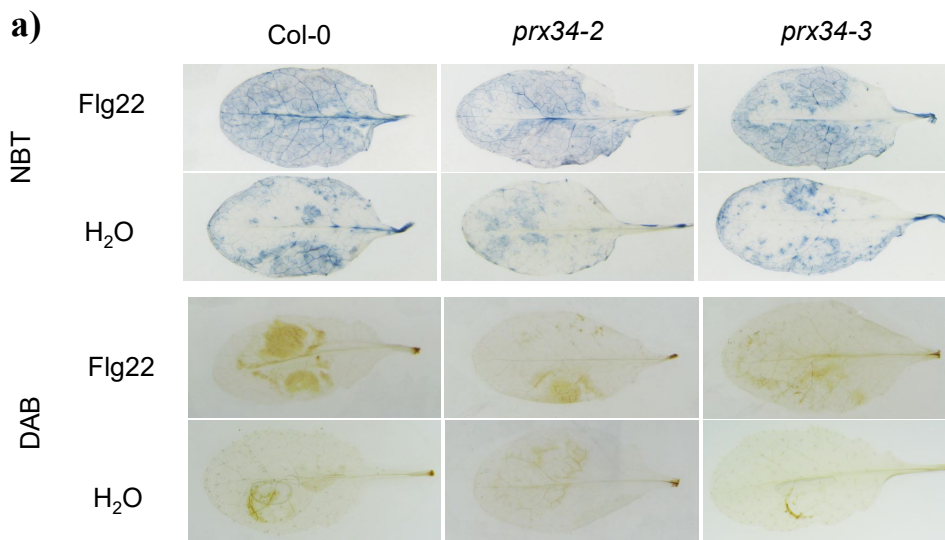


**Figure 3.3** Response of *prx34-1* and *prx34-2* mutants to Flg22. **(a)** Flg22-elicited ROS generation in Arabidopsis leaves. Approximately 0.1 ml of 100 nM Flg22 or water (as control) were infiltrated into mature leaves of 4-week-old seedlings of the wild-type, *prx34-2* and *prx34-3*. The leaves were stained with Nitroblue tetrazolium (NBT) at 1 h after treatment to detect the accumulation of superoxide and 3,3'-diaminobenzidine (DAB) at 2 h after treatment to detect the accumulation of H<sub>2</sub>O<sub>2</sub>, respectively. Experiments were repeated three times with similar results. **(b)** Flg22-elicited callose accumulation detected by aniline blue staining. Approximately 0.1 ml of 100 nM Flg22 or water (as control) were infiltrated into mature leaves as described above. The leaves were stained with aniline blue at 24 h after treatment to detect callose accumulation. The number of callose was calculated using an ImageJ software. Data represent the average  $\pm$  SD of ten leaves from 5 independent plants Asterisks indicate significant difference (Dunnett's test; \*\*\*,  $p < 0.001$ ).

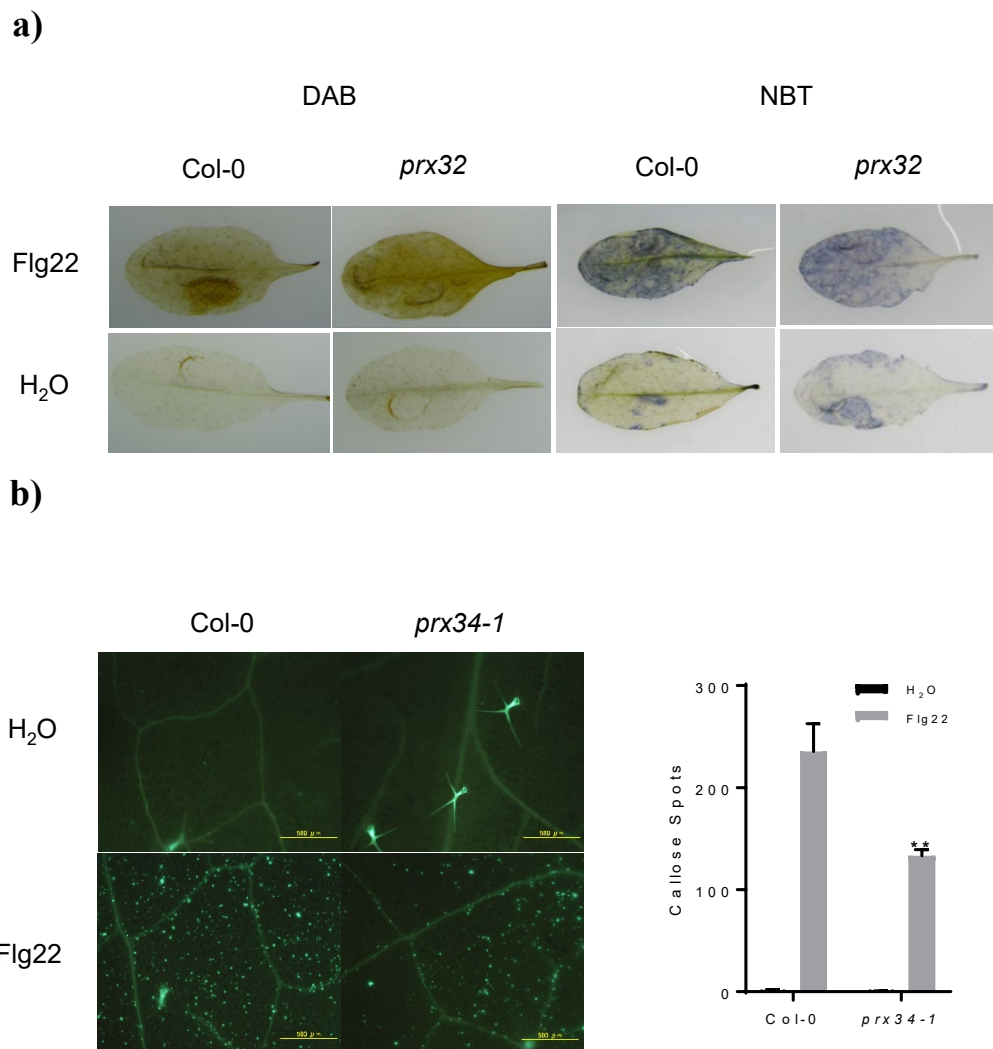


**Figure 3.4** Response of *prx32* and *prx34-1* mutants to Flg22. **(a)** Flg22-elicited ROS generation in Arabidopsis leaves. Approximately 0.1 ml of 100 nM Flg22 or water (as control) were infiltrated into mature leaves of 4-week-old seedlings of the wild-type and *prx32*. The leaves were stained with Nitroblue tetrazolium (NBT) at 1 h after treatment to detect the accumulation of superoxide and 3,3'-diaminobenzidine (DAB) at 2 h after treatment to detect the accumulation of H<sub>2</sub>O<sub>2</sub>, respectively. Experiments were repeated three times with similar results. **(b)** Flg22-elicited callose accumulation detected by aniline blue staining. Approximately 0.1 ml of 100 nM Flg22 or water (as

control) were infiltrated into mature leaves as described above. The leaves were stained with aniline blue at 24 h after treatment to detect callose accumulation. The number of callose was calculated using an ImageJ software. Data represent the average  $\pm$  SD of ten leaves from 5 independent plants Asterisks indicate significant difference (Dunnett's test; \*\*\*,  $p < 0.001$ ).

### 3.5 Discussion

PRXs function in the plant defense response by consuming H<sub>2</sub>O<sub>2</sub> through the peroxidase cycle for cell wall cross-linking or lignification to block pathogen ingress or by producing ROS through the oxidative cycle during the PAMP-triggered oxidative burst (Bolwell et al., 2002; O'Brien et al., 2012a). PRXs can directly generate H<sub>2</sub>O<sub>2</sub> from O<sub>2</sub> in the presence of a still unknown reductant and upon extracellular alkalinization, which typically occurs upon PAMP perception.

Here, we provide several lines of evidence that show that Arabidopsis cell wall peroxidases encoded by PRX34 play important roles in PTI elicited in response to Flg22. *prx34-2* and *prx34-3* exhibit a diminished oxidative burst in mature leaves after infiltration with Flg22 and the same failed to elicit callose deposition (Fig. 3.3). *prx34* null mutant plants also exhibited enhanced susceptibility to the *B. cinerea*, *C. higginsianum* and *P. carotovorum* subsp. *carotovorum* strain Pc1. These data indicate a significant defect in Flg22-mediated signaling in mature PRX34 knockdown plants, and explanation for why these plants are more susceptible to pathogens is that they are impaired in PTI.

PRXs function in the plant defense response by consuming H<sub>2</sub>O<sub>2</sub> through the peroxidase cycle for cell wall cross-linking or lignification to block pathogen ingress or by producing ROS through the oxidative cycle during the PAMP-triggered oxidative burst (Bolwell et al., 2002; O'Brien et al., 2012a). PRXs can directly generate H<sub>2</sub>O<sub>2</sub> from O<sub>2</sub> in the presence of a still unknown reductant and upon extracellular alkalinization, which typically occurs upon PAMP perception.

# **Chapter IV**

## **Overexpression of *PRX34* Enhance Flg22-elicited Immune Responses and Confers Resistance to Pathogens**

## 4.1 Abstract

Two independent lines of *Arabidopsis* plants expressing the *PRX34* under the control of the CaMV35S promoter, named OX #3-3 and OX #8-1, were used to further define the function of *PRX34*. The overexpression lines exhibited normal growth similar to the wild-type. Western blot analysis with NaCl-solubilized extracts recovered from the wild-type, the OX #3-3 and OX #8-1 plants revealed more accumulation of corresponding peroxidase, consistent with the transcript analysis. Consistently, the activity that generates ROS in the cell wall extracts of the OX #3-3 and OX #8-1 were constantly higher than the wild-type. Interestingly, *Arabidopsis* plants expressing *PRX34* restricted lesion development compared to the wild-type, when inoculated with virulent strains such as *B. cinerea*, *P. carotovorum* subsp. *carotovorum* and *Pseudomonas syringae* pv. *tomato*. This result is consistent with our finding that increased expression of *PRX34* produced more ROS and callose than the wild-type plants, when infiltrated with Flg22. Finally, using the wild-type and the OX #8-1 plants, leaf disks were exposed to 100 nM of Flg22 in a solution containing 200  $\mu$ M L-012, in the absence or presence of diphenylene iodonium (DPI), a chemical inhibitor of NADPH oxidase, to ascertain the role of peroxidase in early oxidative burst. Although no obvious difference in the Flg22-elicited oxidative burst was observed between the wild-type and the OX #8-1, the ROS burst occurred more rapidly in the #8-1, suggesting a role of increased *PRX34* in early oxidative burst. Indeed, due to increased *PRX34* expression, the OX #8-1 produced DPI-insensitive ROS compared to the wild-type.

## 4.2 Introduction

### 4.2.1 *Pseudomonas syringae* pv. *tomato* strain DC3000

As a species, *Pseudomonas syringae* causes economically important diseases in a wide range of plant species. However, each strain may exhibit a high degree of host specificity and infect only a limited number of plant species or even a few cultivars of a single plant species. This specificity is the basis of grouping *P. syringae* strains into pathovars (pv.). Currently, approximately 50 pathovars are recognized (Gardan et al. 1999), and each pathovar can be further divided into multiple races on the basis of differential interactions with cultivars of a plant species.

*P. syringae* may be best described as a locally infecting, hemibiotrophic pathogen. It infects mainly aerial portions of plants, such as leaves and fruits. Infection is often contained within a few millimeters of the initial infection sites and does not spread to other parts of the plant. In a successful disease cycle, *P. syringae* strains generally live two lifestyles that are spatially and temporally interconnected: an initial epiphytic phase upon arrival on the surface of a healthy plant and an endophytic phase in the apoplastic space after entering the plant through natural openings and accidental wounds (Beattie and Lindow 1995; Hirano and Upper 2000; Melotto and Underwood 2008). Under favorable environmental conditions (e.g., heavy rain, high humidity, moderate temperature), *P. syringae* can multiply very aggressively in a susceptible host plant. The most aggressive phase of *P. syringae* multiplication in planta occurs in the absence of apparent host cell death. However, at the late stage of pathogenesis (often

after bacteria have almost reached the peak population in the infected tissues), host cells die and infected tissues show extensive necrosis. This pathogenesis mode is distinct from that of strictly biotrophic pathogens, which obtain nutrients from living host cells without causing host cell death, and from that of strictly necrotrophic pathogens, which kill host cells during early stages of infection as the main strategy of obtaining nutrients. *Pseudomonas syringae* pv. *tomato* is the causal agent of bacterial speck of tomato. *P. syringae* pv. *tomato* DC3000 is a model strain for investigating plant-microbe interactions due to its genetic tractability and pathogenicity on tomato, *Arabidopsis*, and *Brassica* spp. (Cuppels 1986; Elizabeth and Bender 2007; Whalen et al. 1991). *P. syringae* pv. *tomato* causes necrotic lesions on the leaves, stems, and fruit of tomato plants (Goode and Sasser 1980). The necrotic and chlorotic symptoms produced by *P. syringae* pv. *tomato* on host plants are quite distinctive, although they are occasionally confused with the symptoms of bacterial leaf spot caused by *Xanthomonas campestris* pv. *vesicatoria*.

#### **4.2.2 Luminol L-012**

L-012 (8-amino-5-chloro-7-phenyl-pyrido[3,4-d] pyridazine-1,4(2H,3H) dione) is a luminol-based molecule that has been reported to produce much stronger chemiluminescence (CL) than other CL probes (lucigenin, luminol, and MCLA) (Nishinaka et al. 1993; Sohn et al. 1999). Thus, L-012 is rapidly emerging as a popular CL probe for measuring superoxide ( $O_2^{\cdot -}$ ) and other reactive oxygen species (ROS) derived particularly from NADPH oxidases (Ambasta et al. 2006; Judkins et al. 2010;

Daiber et al. 2004 and Ichibangase et al. 2013). In an earlier report, investigators concluded that unlike other CL probes, L-012 is not subject to redox cycling and is, therefore, reliable for detecting Nox-derived  $O_2^{\cdot-}$  inhibitors in high throughput screening (HTS) assays (Daiber et al. 2004). More recently, L-012 was used to noninvasively image ROS and reactive nitrogen species (RNS) in living mice under pro-inflammatory conditions (Kielland et al. 2009; Han et al. 2012).

## **4.3 Materials and Methods**

### **4.3.1 Plant Materials and Growth Conditions**

For the overexpression experiment, we amplified the open reading frame of the *PRX34* by RT-PCR with complementary DNA from Arabidopsis seedlings, cloned it downstream of the CaMV 35S promoter in pENTR4m (Matsui et al. 2017) using an In-Fusion HD Cloning Kit (Clontech), and subsequently recloned into a binary vector pGWB2 (Nakagawa et al. 2007) using LR clonase II enzyme mix (Thermo Fisher Scientific). Two independent transgenic Arabidopsis plants were generated by the standard floral dip method (Clough and Bent 1998).

### **4.3.2 RNA Extraction and Quantitative RT-PCR Analysis**

RNA extraction and quantitative RT-PCR analysis was described in Chapter 2.

### **4.3.3 Infection Assays**

*Pseudomonas syringae* pv. *tomato* DC3000 was grown in 5 ml liquid King's broth (KB) medium overnight at 28°C, washed twice with 10 mM  $MgSO_4$ , and then

resuspended in 10 mM MgSO<sub>4</sub> supplemented with 0.025% silwet. The amount of bacteria was adjusted to  $1 \times 10^7$  cfu/ml and sprayed onto 4-week-old plants. The plants were covered with plastic lids to keep the moisture level high. At the indicated time points, two leaves were obtained from each plant, and a 0.5 cm<sup>2</sup> leaf disk was harvested at each site of infection. The samples from one plant were combined to form one biological sample. The number of viable bacteria in each biological sample was then determined by counting cfus.

For *B. cinerea* and *P. carotovorum* subsp. *carotovorum* was described in Chapter 3.

#### **4.3.4 Detection of Reactive Oxygen Species**

Detection of reactive oxygen species was described in Chapter 3.

#### **4.3.5 Assay for Callose Formation**

Assay for callose formation was described in Chapter 3.

#### **4.3.6 Chemiluminescence detection of the oxidative burst in plant leaf pieces**

Kinetic analysis of ROS generated in the wild-type and the OX #8-1 in the absence or presence of diphenylene iodonium (DPI), a chemical inhibitor of NADPH oxidase. Leaf disks were exposed to 100 nM of Flg22 in a solution containing 200  $\mu$  M L-012 (Fujifilm Wako Pure Chemical Co.Ltd., Osaka, Japan), in the absence or presence of DPI.

## 4.4 Results

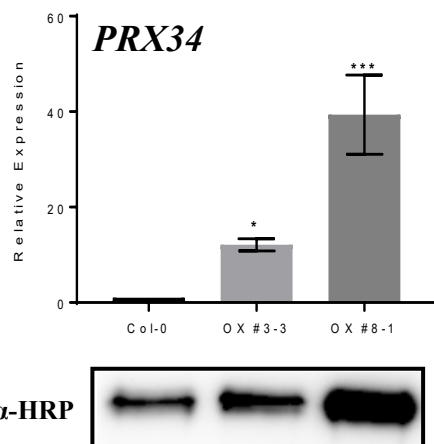
### 4.4.1 Identification of two independent *35S:PRX34*-overexpressing lines

To further define the function of PRX34, we generated two independent lines of *Arabidopsis* plants expressing the PRX34 under the control of the CaMV 35S promoter. The overexpression lines, named OX #3-3 and OX #8-1 exhibited normal growth similar to the wild-type (Fig. 4.1a). Western blot analysis with NaCl-solubilized extracts recovered from the wild-type, OX #3-3 and OX #8-1 plants revealed more accumulation of corresponding peroxidase, consistent with the transcript analysis (Fig. 3b). Actually, the activity that generates ROS in the cell wall extracts of the OX #3-3 and OX #8-1 were higher than the wild-type (Fig. 4.1b).

a)



b)



c)

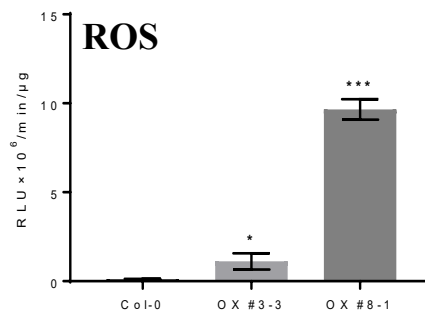


**Figure 4.1** Characterization of *35S:PRX34* overexpression line in *Arabidopsis thaliana* (Col). (a) Growth of 4 week-old seedlings of two *PRX34*-overexpressors, OX #3-3 and OX #8-1. (b) *PRX34* transcript levels in mature leaves of 4-week old seedlings of the wild-type, OX #3-3 and OX #8-1. The inset shows accumulation of peroxidase proteins probed with anti-HRP antibody. (c) Generation of ROS in cell wall extracts through NADH oxidation. The cell wall proteins (0.25  $\mu$ g) from individual plants were incubated in a reaction mixture (50  $\mu$ l) containing 30 mM Tris/MES (pH 6.5), 0.5 mM NADH, 0.5 mM *p*-coumaric acid (*p*-CA) and 20 mM MnCl<sub>2</sub> and 10  $\mu$ M MPEC (ATTO Co.,Ltd., Tokyo, Japan). Chemiluminescence (RLU) was measured with a Lumat

LB9507 (Berthold Technologies, Bad Wildbad, Germany) for 2 min. Data represent the average  $\pm$  SD of three replicates. Asterisks indicate significant difference (Dunnett's test; \*\*\*,  $p < 0.001$ ).

#### **4.4.2 Overexpression of *PRX34* confers resistance to virulent strains *B. cinerea*, *P. carotovorum* subsp. *carotovorum* and *Pseudomonas syringae* pv. *tomato***

To explore the potential effect of the enhanced expression of *PRX34* in disease resistance, we infected OX#3-3, OX #8-1 and wild-type plants with two necrotrophic pathogens, the soft-rot bacterium *P. carotovorum* subsp. *carotovorum* strain Pc1, the gray mold fungus *B. cinerea*, and the hemibiotroph *P. syringae* pv. *tomato* DC3000. Interestingly, Arabidopsis plants expressing *PRX34* restricted lesion development compared to the wild-type plants (Fig. 4.2). These results indicate that the overexpression of *PRX34* in OX#3-3 and OX #8-1 lines prime plant defenses to the pathogens.

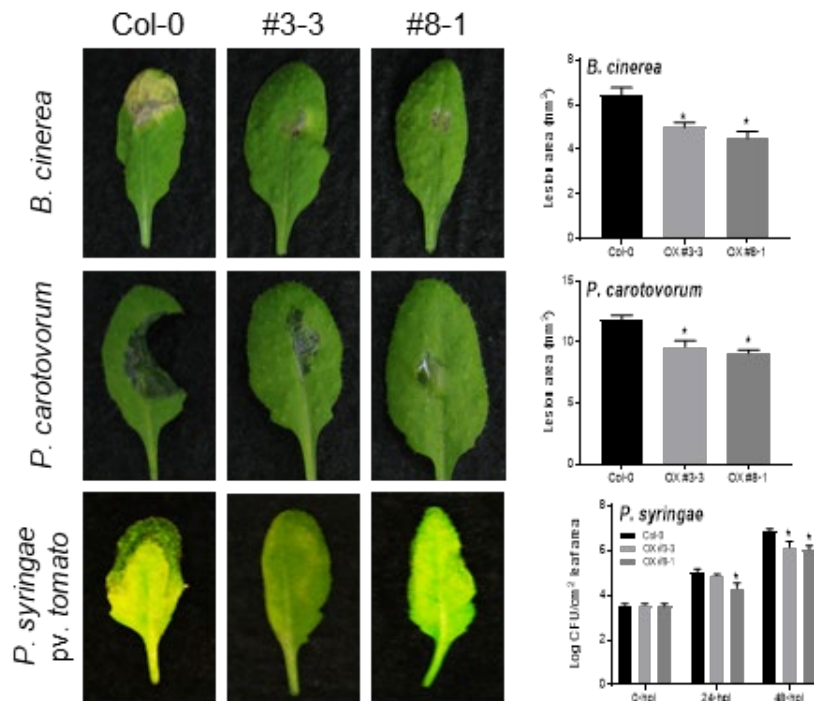


**Figure 4.2** Overexpression of *PRX34* caused enhanced resistance to virulent strains of fungal and bacterial pathogens. *B. cinerea* was inoculated by placing 5- $\mu$ l drop of a suspension ( $2 \times 10^5$  conidia/ml) in 1% Sabouraud Maltose Broth onto both side of the middle vein of the detached leaves of 4-week-old wild-type, OX #3-3 and OX #8-1. For inoculation with *P. carotovorum* subsp. *carotovorum* strain Pc1, 5- $\mu$ l drop of a bacterial suspension ( $1 \times 10^5$  cfu/ml) was placed onto injured leaves. For inoculation with *P. syringae* pv. *tomato* DC3000, leaves of the wild-type, OX #3-3 and OX #8-1 were infiltrated with a bacterial suspension ( $1 \times 10^7$  cfu/ml). Bacterial cells were counted 1 and 2 days after inoculation. All inoculated leaves were incubated for 2 or 3 days at 22°C before taking photos and measuring the lesion size. Data are shown as the mean of bacterial titers  $\pm$  SD of eight leaf disks excised from 8 leaves of 4 independent plants. Asterisk indicates significant difference (Dunnett's test; \*,  $p < 0.05$ ).

#### **4.4.3 Overexpression of *PRX34* are enhanced in Flg22-elicited immune responses**

To explore the overexpression of *PPRX34* contribute to the PTI response, we treated plants with Flg22 peptide (Fig. 4.3). Consistent with the enhanced resistance to pathogens, OX #3-3 and OX #8-1 exhibit enhanced PTI-responses, such as an increase in the accumulation of  $O_2^-$  and  $H_2O_2$  (Fig. 4.3a), and more callose deposition (Fig. 4.3b). These results clearly indicated that the increased expression of *PRX34* was indeed responsible for the Flg22-elicited immune responses.

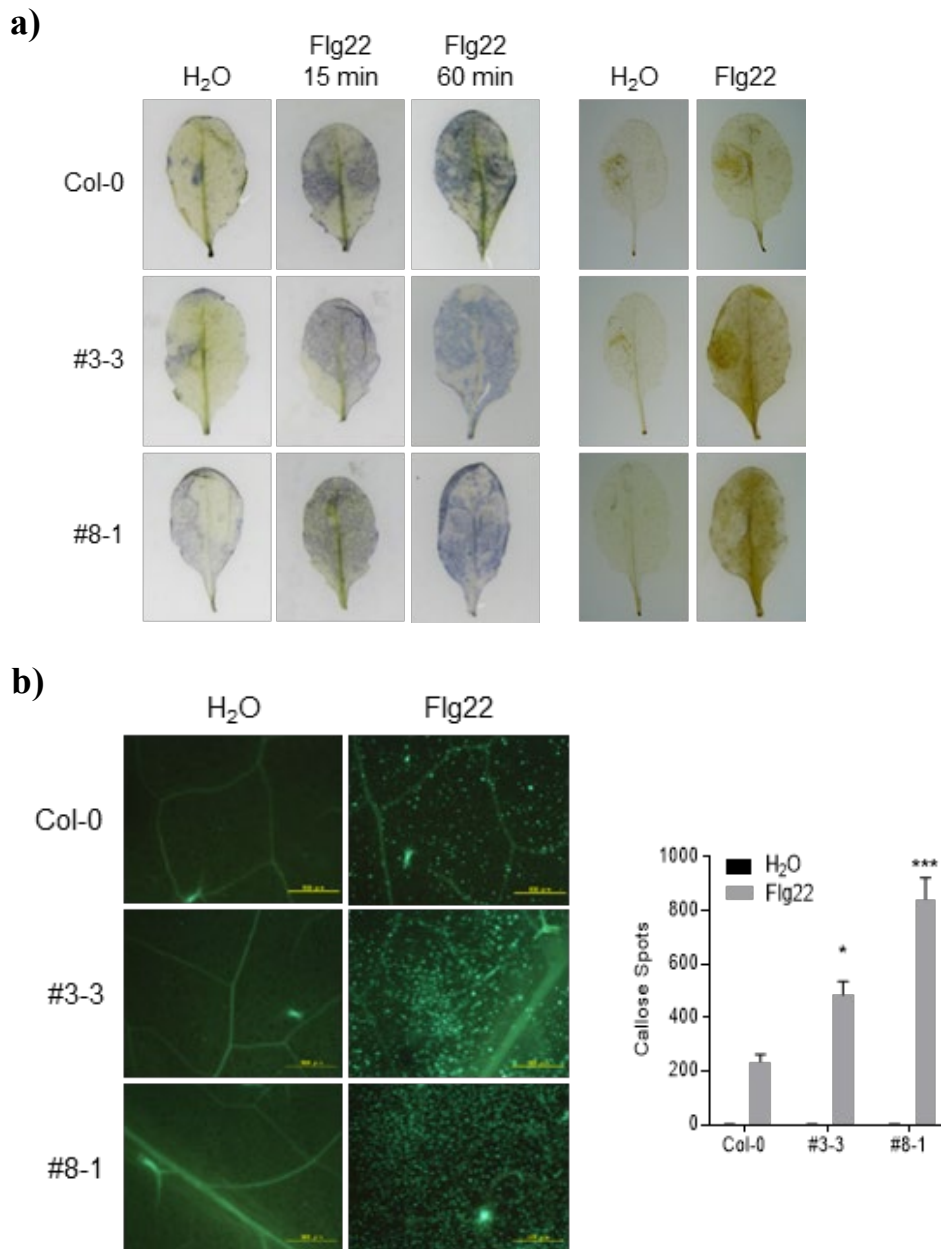


**Figure 4.3** Detection of *PRX34*-overexpression lines in response to Flg22. **(a)** NBT and DAB staining to detect superoxide ( $O_2^-$ ) and  $H_2O_2$ , respectively. Leaves of 4 week-old plants of the wild-type, OX#3-3 and OX #8-1 were treated with 100 nM Flg22 or water (as control). Respective staining was performed for 15 or 60 min after treatment. Experiments were repeated at three times with similar results. **(b)** Callose accumulation in Flg22-treated leaves of the wild-type and two *PRX34*-overexpressors, OX #3-3 and

OX #8-1. Leaves were treated with 100 nM of Flg22 or water (as control) for 24 h similarly and then stained with aniline blue to detect callose accumulation. The number of callose was calculated using an ImageJ software. Data represent the average  $\pm$  SD of ten leaves from 5 independent plants Asterisks indicate significant difference (Dunnett's test; \*,  $p < 0.05$ ; \*\*\*,  $p < 0.001$ ).

#### **4.4.4 Detection of the ROS-burst in plant leaf pieces using a luminol-based bioassay**

Finally, using the wild-type and the OX #8-1 plants, leaf disks were exposed to 100 nM of Flg22 in a solution containing 200  $\mu$  M L-012, in the absence or presence of diphenylene iodonium (DPI), a chemical inhibitor of NADPH oxidase, to ascertain the role of peroxidase in early oxidative burst. Although no obvious difference in the Flg22-elicited oxidative burst was observed between the wild-type and the OX #8-1, the ROS burst occurred more rapidly in the #8-1 (Fig. 4c), suggesting a role of increased PRX34 in early oxidative burst. Indeed, due to increased PRX34 expression, the OX #8-1 produced DPI-insensitive ROS compared to the wild-type (Fig. 4c). This was also confirmed by a statistical analysis of integrated values of relative light value (RLU) over 3600 seconds after each treatment; the value 176 of the Flg22-elicited OX #8-1 with DPI was constantly higher than that of the wild-type (Fig. 4d).

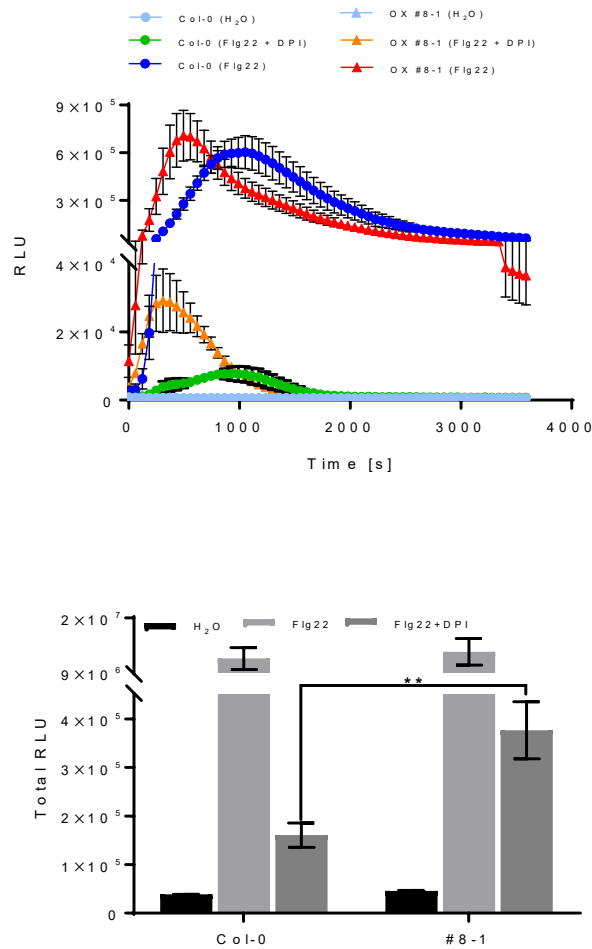


**Figure 4.4** Kinetic analysis of ROS generated in the wild-type and the OX #8-1 in the absence or presence of diphenylene iodonium (DPI), a chemical inhibitor of NADPH oxidase. Leaf disks were exposed to 100 nM of Flg22 in a solution containing 200  $\mu$  M L-012 (Fujifilm Wako Pure Chemical Co.Ltd., Osaka, Japan), in the absence or presence of DPI. ROS generated in the test solution was measured successively with a TriStar2 LB942 (Berthold Technologies, Bad Wildbad, Germany) for 60 min. Data are means  $\pm$  SD from three biological replicates. d) A statistical analysis of integrated values of relative light value (RLU) over 3600 seconds after each treatment described in the Fig. 4c. Asterisks indicate significant difference (Dunnett's test; \*\*,  $p < 0.01$ ).

## 4.5 Discussion

The enhanced PTI responses to Flg22 is the simplest explanation for why overexpression of *PRX34* confer resistance to Pst DC3000, *B. cinerea* and *P. carotovorum* in OX# 3-3 and OX# 8-1. It was previous demonstrated that *PRX33* and *PRX34* play important roles in Arabidopsis PTI responses (Bindschedler et al., 2006; Daudi et al., 2012), but the respective roles of PRX33 and PRX34 are still elusive. PRXs consuming H<sub>2</sub>O<sub>2</sub> through the peroxidase cycle for cell wall cross-linking or lignification to block pathogen access or by producing ROS through the oxidative cycle during the PAMP-triggered oxidative burst (Bolwell et al., 2002; O'Brien et al., 2012a). Furthermore, *PRX33* and *PRX34*, but not the *NADPH* oxidases *RBOHD* and *RBOHF*, were demonstrate that regulate SA- and PAMP-mediated stomatal defensive response through the production of ROS (Arnaud et al., 2017). In Arabidopsis, overexpressing selected class III peroxidase gene lead to increase resistance to necrotrophic phytopathogen *B. cinerea* and *P. carotovorum* through regulation of OG (oligogalacturonide) signaling pathway, and these results further support that class III peroxidases are implicate in immunity response to necrotrophic pathogens.

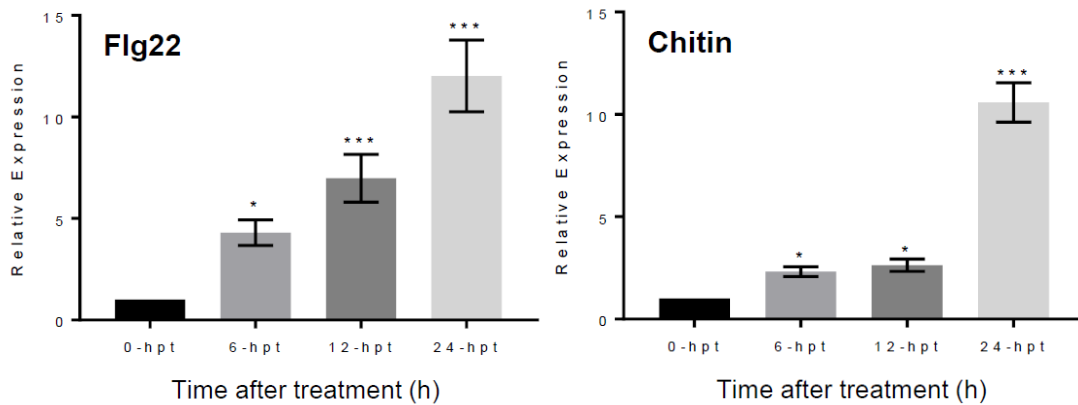


**Figure 5** Induction of *PRX34* transcript levels in Arabidopsis in response to Flg22 or chitoheptaose. Approximately 0.1 ml of 100 nM Flg22, 100  $\mu$ g/ml chitoheptaose or water (as control) were infiltrated into mature leaves of 4-week-old seedlings of the wild-type. Flg22 peptide and chitoheptaose (GLU437) were obtained from GenScript (Piscataway, NJ, USA) and Elicityl (Crolles, France), respectively. Leaves were harvested at 6, 12 and 24 h after infiltration, then subjected to quantitative RT-PCR with a Shimadzu GVP-9600 Gene Detection S 451 system (Shimadzu, Kyoto, Japan), using primers listed in Table 2.2. The expression level of the *PRX34* was normalized by the *EF1- $\alpha$*  gene (*At1g07920*) and was expressed relative to the water-treated control sample. Data are shown as the average  $\pm$  standard deviation (SD) from three independent plants. Asterisk indicate statistically significant difference (Dunnett's test; \*,  $p < 0.05$ ; \*\*\*,  $p < 0.001$ ).

## SUMMARY

In this study, we evaluated the role of Arabidopsis class III PRX34 especially in terms of Flg22-elicited oxidative burst and callose formation as early (~10 min) and late (~24 hours) responses, respectively. Arabidopsis plants lacking PRX34 almost completely abolished the Flg22-elicited callose (Fig. 4c). Importantly, both *prx34-2* and *prx34-3* plants caused enhanced susceptibility to virulent pathogens, whereas ectopic expression of *PRX34* improved resistance (Figs. 3a and 4a). Mammarella et al. (2015) reported recently that in Arabidopsis, SA-mediated activation of *PR1* was impaired in *PRX34*-silenced plants. Furthermore, the expression of defense-related genes such as *PR1*, *WRKY38* and *WRKY54* following infection with a virulent strain of *P. syringae* pv. *tomato* was clearly diminished when *PRX34* was silenced. Taken together, our results suggest that certain isoform(s) such as PRX34 substantially contributes to both early and late responses during PTI. Indeed, PRX34 was shown to be upregulated upon infection or in response to elicitor such as Flg22 and chitin (Bindschedler et al. 2006; Daudi et al. 2012; Figure 5). Therefore, both constitute and induced peroxidases play important role during PTI. Further experiments are needed to explore the distinctive roles of plant class III peroxidase(s) in the early oxidative burst, as well as the late responses including downstream defense-signaling pathway during PTI.

## REFERENCES

- Almagro L, Gómez RLV., Belchi-Navarro S, Bru R., Ros BA, Pedreño M A (2009) Class III peroxidases in plant defence reactions. *J Exp Bot* 60: 377-390
- Alonso JM, Stepanova AN, Leisse TJ, Kim CJ, Chen H, Shinn P, Stevenson DK, Zimmerman J, Barajas P, Cheuk R, Gadrinab C, Heller C, Jeske A, Koesema E, Meyers CC, Parker H, Prednis L, Ansari Y, Choy N, Deen H, Geralt M, Hazari N, Hom E, Karnes M, Mulholland C, Ndubaku R, Schmidt I, Guzman P, Aguilar-Henonin L, Schmid M, Weigel D, Carter DE, Marchand T, Risseuw E, Brogden D, Zeko A, Crosby WL, Berry CC, Ecker JR (2003) Genome-wide insertional mutagenesis of *Arabidopsis thaliana*. *Science* 301: 653-657
- Alvarez ME, Pennell RI, Meijer PJ, Ishikawa A, Dixon RA, Lamb C (1998) Reactive oxygen intermediates mediate a systemic signal network in the establishment of plant immunity. *Cell* 92:773–784
- Ambasta RK, Schreiber JG, Janiszewski M, Busse R, Brandes RP. (2006) Nox1 is a central component of the smooth muscle NADPH oxidase in mice. *Free Radic Biol Med.* 41:193–201.
- Apostol I, Heinsteins PF, Low PS (1989) Rapid stimulation of an oxidative burst during elicitation of cultured plant cells: role in defense and signal transduction. *Plant Physiol* 90:109–116
- Arnaud D, Lee S, Takebayashi Y, Choi D, Choi J, Sakakibara H, Hwang I (2017) Cytokinin-mediated regulation of reactive oxygen species homeostasis modulates

- stomatal immunity in Arabidopsis. *Plant Cell* 29: 543-559
- Bach M, Schnitzler JP, Seitz HU (1993) Elicitor-induced changes in Ca<sup>++</sup> influx, K<sup>+</sup> efflux, and 4-hydroxybenzoic acid synthesis in protoplasts of *Daucus carota* L. *Plant Physiol* 103:407–412
- Baker CJ, Orlandi EW (1995) Active oxygen in plant pathogenesis. *Annu Rev Phytopathol* 33:299–321
- Bartz, J. A. (1991). *Compendium of Tomato Diseases*. American Phytopathological Society, St. Paul, MN. 44-45.
- Beattie GA, Lindow SE. (1995). The secret life of foliar bacterial pathogens on leaves. *Annu. Rev. Phytopathol.* 33: 145–72
- Bellincampi, D., Cervone, F., and Lionetti, V. (2014) Plant cell wall dynamics and wall-related susceptibility in plant-pathogen interactions. *Front. Plant Sci.* 5:228.
- Berglund GI, Carlsson GH, Smith AT, Szoke H, Henriksen A, Hajdu J (2002) The catalytic pathway of horseradish peroxidase at high resolution. *Nature* 417:463–468
- Bestwick C, Brown I, Mansfield J (1998) Localized changes in peroxidase activity accompany hydrogen peroxide generation during the development of a nonhost hypersensitive reaction in lettuce. *Plant Physiol* 118:1067–1078
- Bindschedler L, Dewdney J, Blee K, Stone J, Asai T, Plotnikov J, Denoux C, Hayes T, Gerrish C, Davies D (2006) Peroxidase-dependent apoplastic oxidative burst in Arabidopsis required for pathogen resistance. *Plant J* 47:851–863
- Bittel, P., and Robatzek, S. (2007) Microbe-associated molecular patterns (MAMPs) probe plant immunity. *Curr. Opin. Plant Biol.* 10, 335–341.

Blancard, D., Lecoq, H., and Pitrat, M. (1994). A Colour Atlas of Cucurbit Diseases: Observation, Identification & Control. Manson Publishing, London.125, 143, 183.

Bolwell GP, Bindschedler LV, Blee KA, Butt VS, Davies DR, Gardner SL, Gerrish C, Minibayeva F (2002) The apoplastic oxidative burst in response to biotic stress in plants: a three component system. *J Exp Bot* 53: 1367-1376

Bolwell GP, Blee KA, Butt VS, Davies DR, Gardner SL, Gerrish C, Minibayeva F, Rowntree EG, Wojtaszek P (1999) Recent advances in understanding the origin of the apoplastic oxidative burst in plant cells. *Free Radic Res* 31(Suppl):S137–S145

Bolwell GP, Butt VS, Davies DR, Zimmerlin A (1995) The origin of the oxidative burst in plants. *Free Radic Res* 23:517–532

Bolwell GP, Davies DR, Gerrish C, Auh CK, Murphy TM (1998). Comparative biochemistry of the oxidative burst produced by rose and French bean cells reveals two distinct mechanisms. *Plant Physiol* 116: 1379-1385

Brown I, Trethowan J, Kerry M, Mansfield J, Bolwell GP (1998) Localization of components of the oxidative cross-linking of glycoproteins and of callose synthesis in papillae formed during the interaction between non-pathogenic strains of *Xanthomonas campestris* and French bean mesophyll cells. *Plant J* 15:333–343

Chaouch S, Queval G, Noctor G (2012) AtRbohF is a crucial modulator of defence-associated metabolism and a key actor in the interplay between intracellular oxidative stress and pathogenesis responses in Arabidopsis. *Plant J* 69:613–627

Choi HW, Kim YJ, Lee SC, Hong JK, Hwang BK (2007) Hydrogen peroxide generation by the pepper extracellular peroxidase CaPO2 activates local and systemic

cell death and defense response to bacterial pathogens. *Plant Physiol* 145:890–904

Clough SJ, Bent AF (1998) Floral dip: a simplified method for *Agrobacterium*-mediated transformation of *Arabidopsis thaliana*. *Plant J* 16: 735-743

Crouch J., O’Connell R., Gan P., Buiate E., Torres M.F., Beirn L., Shirasu K., Vaillancourt L. The genomics of *Colletotrichum*. In: Dean R.A., Lichens-Park A., Kole C., editors. *Genomics of Plant-Associated Fungi: Monocot Pathogens*. Springer; Berlin, Germany: 2014. pp. 69–102.

Cuppels, D. (1986). Generation and characterization of Tn5 insertion mutations in *Pseudomonas syringae* pv. tomato. *Appl. Environ. Microbiol.* 51:323-327.

Daiber A, August M, Baldus S, Wendt M, Oelze M, Sydow K, Kleschyov AL, Munzel T. (2004) Measurement of NAD(P)H oxidase-derived superoxide with the luminol analogue L-012. *Free Radic Biol Med.* 36:101–111.

Damm U., O’Connell R.J., Groenewald J.Z., Crous P.W. The *Colletotrichum destructivum* [italicize] species complex—hemibiotrophic pathogens of forage and field crops. *Stud. Mycol.* 2014; 79:49–84.

Dangl JL, Horvath DM, Staskawicz BJ. (2013). Pivoting the plant immune system from dissection to deployment. *Science* 341, 746–51.

Daudi A, Cheng Z, O’Brien JA, Mammarella N, Khan S, Ausubel FM, Bolwell GP (2012) The apoplastic oxidative burst peroxidase in *Arabidopsis* is a major component of pattern-triggered immunity. *Plant Cell* 24: 275-287

Davies DR, Bindschedler LV, Strickland TS, Bolwell GP (2006) Production of reactive oxygen species in *Arabidopsis thaliana* cell suspension cultures in response to

an elicitor from *Fusarium oxysporum*: implication for basal resistance. *J Exp Bot* 57: 1817-1827

De Silva D.D., Crous P.W., Ades P.K., Hyde K.D., Taylor P.W. Life styles of *Colletotrichum* species and implications for plant biosecurity. *Fungal Biol. Rev.* 2017; 31:155–168.

Desikan R, Neill SJ, Hancock JT (2000) Hydrogen peroxide-induced gene expression in *Arabidopsis thaliana*. *Free Radic Biol Med* 28:773–778

Devlin WS, Gustine DL (1992) Involvement of the oxidative burst in phytoalexin accumulation and the hypersensitive reaction. *Plant Physiol.* 100, 1189–1195

Dodds PN, Rathjen JP. (2010). Plant immunity: towards an integrated view of plant-pathogen interactions. *Nature Reviews in Genetics.* 11, 539–48.

Droby, A. and Lichter, A. (2004) Post-harvest *Botrytis* infection: etiology, development and management. In: *Botrytis: Biology, Pathology and Control.* (Elad, Y., Williamson, B., Tudzynski, P. and Delen, N., eds), pp. 349–367. Dordrecht, The Netherlands: Kluwer Academic Press.

Dunford B (1993) Kinetics of peroxides reactions: horseradish, barley, *Corpinus cinereus*, lignin and manganese. In: Welinder KG, Rasmussen S, Penel C, Greppin H (eds) *Plant peroxidases: biochemistry and physiology.* University of Geneva, Geneva, pp 113–124

Elizabeth, S. V., and Bender, C. L. (2007). The phytotoxin coronatine from *Pseudomonas syringae* pv. tomato DC3000 functions as a virulence factor and influences defense pathways in edible Brassicas. *Mol. Plant Pathol.* 8:83-92.

- Espinosa, A., and Alfano, J. R. (2004). Disabling surveillance: bacterial type III secretion system effectors that suppress innate immunity. *Cell. Microbiol.* 6, 1027–1040.
- Feldmann, K.A. (1991) T-DNA insertion mutagenesis in *Arabidopsis* mutational spectrum. *The Plant Journal*.1: 71-82.
- Felix G, Regenass M, Boller T (1993) Specific perception of subnanomolar concentrations of chitin fragments by tomato cells: induction of extracellular alkalinization, changes in protein phosphorylation, and establishment of a refractory state. *Plant J.* 4, 307–316
- Ferrari, S., Savatin, D. V., Sicilia, F., Gramegna, G., Cervone, F., and Lorenzo, G. D. (2013). Oligogalacturonides: plant damage-associated molecular patterns and regulators of growth and development. *Front. Plant Sci.* 4, 49.
- Gardan L, Gouy C, Christen R, Samson R. (2003). Elevation of three subspecies of *Pectobacterium carotovorum* to species level: *Pectobacterium atrosepticum* sp. nov., *Pectobacterium betavascularum* sp. nov. and *Pectobacterium wasabiae* sp. nov. *Int. J. Syst. Evol. Microbiol.* 53: 381-391.
- Gardan L, Shafik H, Belouin S, Broch R, Grimont F, Grimont PA. (1999). DNA relatedness among the pathovars of *Pseudomonas syringae* and description of *Pseudomonas tremae* sp. nov. and *Pseudomonas cannabina* sp. nov. (ex Sutic and Dowson 1959). *Int. J. Syst. Bacteriol.* 49(2):469–78
- Gomez-Gomez L, Boller T (2000) FLS2: an LRR receptor-like kinase involved in the perception of the bacterial elicitor flagellin in *Arabidopsis*. *Mol Cell.* 5, 1003–1011

- Goode, M. J., and Sasser, M. 1980. Prevention—The key to controlling bacterial spot and bacterial speck of tomato. *Plant Dis.* 64:831-834.
- Grant, J. J., Yun, B.-W., and Loake, G. J. (2000). Oxidative burst and cognate redox signalling reported by luciferase imaging: identification of a signal network that functions independently of ethylene, SA and Me-JA but is dependent on MAPKK activity. *Plant J.* 24, 569–582.
- Gross GG, Janse C, Elstner EF (1977) Involvement of malate, monophenols, and the superoxide radical in hydrogen peroxide formation by isolated cell walls from horseradish (*Armoracia lapathifolia* Gilib.). *Planta* 136: 271-276
- Halliwell B (1978) Lignin synthesis: the generation of hydrogen peroxide and superoxide by horseradish peroxidase and its stimulation by manganese (II) and phenols. *Planta* 140: 81-88
- Han W, Li H, Segal BH, Blackwell TS. (2012) Bioluminescence imaging of NADPH oxidase activity in different animal models. *J Vis Exp.* 68.
- Hirano SS, Upper CD. (2000). Bacteria in the leaf ecosystem with emphasis on *Pseudomonas syringae*: a pathogen, ice nucleus, and epiphyte. *Microbiol. Mol. Biol. Rev.* 64: 624–53
- Hirsch R.E., Lewis B.D., Spalding E.P., Sussman M.R. (1998). A role for AKT1 potassium channel in plant nutrition. *Science* 280, 918–921.
- Hua J., Meyerowitz E.M. (1998). Ethylene responses are negatively regulated by a receptor gene family in *Arabidopsis thaliana*. *Cell* 94, 261–271.
- Ichibangase T, Ohba Y, Kishikawa N, Nakashima K, Kuroda N. (2013) Evaluation of

lophine derivatives as L-012 (luminol analog)-dependent chemiluminescence enhancers for measuring horseradish peroxidase and H<sub>2</sub>O<sub>2</sub>. Luminescence. doi: 10.1002/bio.2513. Epub ahead of print.

Ito Y, Kaku H, Shibuya N (1997) Identification of a high-affinity binding protein for N-acetylchitooligosaccharide elicitor in the plasma membrane of suspension-cultured rice cells by affinity labeling. *Plant J.* 12, 347–356

Jayawardena R.S., Hyde K.D., Damm U., Cai L., Liu M., Li X.H., Zhang W., Zhao W., Yan J.Y. Notes on currently accepted species of *Colletotrichum*. *Mycosphere*. 2016; 7:1192–1260.

Jones JDG, Dangl JL. 2006. The plant immune system. *Nature* 444, 323–9.

Judkins CP, Diep H, Broughton BR, Mast AE, Hooker EU, Miller AA, Selemidis S, Dusting GJ, Sobey CG, Drummond GR. (2010) Direct evidence of a role for Nox2 in superoxide production, reduced nitric oxide bioavailability, and early atherosclerotic plaque formation in ApoE<sup>-/-</sup> mice. *Am J Physiol Heart Circ Physiol*. 298:H24–H32.

Kawano T (2003) Roles of the reactive oxygen species-generating peroxidase reactions in plant defense and growth induction. *Plant Cell Rep* 21: 829-837

Kiba A, Miyake C, Toyoda K, Ichinose Y, Yamada T, Shiraishi T (1997) Superoxide generation in extracts from isolated plant cell walls is regulated by fungal signal molecules. *Phytopathology* 87: 846-852

Kielland A, Blom T, Nandakumar KS, Holmdahl R, Blomhoff R, Carlsen H. (2009) In vivo imaging of reactive oxygen and nitrogen species in inflammation using the luminescent probe L-012. *Free Radic Biol Med*. 47:760–766.

Kimura M, Kawano T (2015) Hydrogen peroxide-independent generation of superoxide catalyzed by soybean p 251 eroxidase in response to ferrous ion. *Plant Signal Behav* 10(11): e1010917. doi: 10.1080/15592324.2015.1010917

Kimura S, Kaya H, Kawarazaki T, Hiraoka G, Senzaki E, Michikawa M, Kuchitsu K (2012) Protein phosphorylation is a prerequisite for the Ca(2+)-dependent activation of Arabidopsis NADPH oxidases and may function as a trigger for the positive feedback regulation of Ca(2+) and reactive oxygen species. *Biochim Biophys Acta* 1823:398–405

Kirschning CJ, Wesche H, Merrill Ayres T, Rothe M (1998) Human toll-like receptor 2 confers responsiveness to bacterial lipopolysaccharide. *J Exp Med* 188:2091–2097

Krysan P.J., Young J.C., Tax F., Sussman M.R. (1996). Identification of transferred DNA insertions within Arabidopsis genes involved in signal transduction and ion transport. *Proc. Natl. Acad. Sci. USA* 93, 8145–8150.

Lamb C, Dixon RA (1997) The oxidative burst in plant disease resistance. *Annu Rev Plant Phys* 48:251–275

Latunde-Dada A.O., O’connell R.J., Nash C., Pring R.J., Lucas J.A., Bailey J.A. Infection process and identity of the hemibiotrophic anthracnose fungus (*Colletotrichum destructivum*) from cowpea (*Vigna unguiculata*) *Mycol. Res.* 1996; 100:1133–1141.

Lee SW, Han SW, Sririyanyum M, Park CJ, Seo YS, Ronald PC (2009) A type I-secreted, sulfated peptide triggers XA21-mediated innate immunity. *Science* 326:850–853

Lemaitre B, Nicolas E, Michaut L, Reichhart JM, Hoffmann JA (1996) The dorsoventral regulatory gene cassette *spatzle/Toll/cactus* controls the potent antifungal response in *Drosophila* adults. *Cell* 86:973–983

Lyons R, Stiller J, Powell, J, Russ A, Manners JM, Kazan K (2015) *Fusarium oxysporum* triggers tissue-specific transcriptional reprogramming in *Arabidopsis thaliana*. *PLoS One* 10(4): e0121902

Macho AP, Zipfel C. 2014. Plant PRRs and the activation of innate immune signaling. *Molecular Cell* 54, 263–72

Mammarella ND, Cheng Z, Fu ZQ, Daudi A, Bolwel, GP, Dong X, Ausubel FM (2015) Apoplastic peroxidases are required for salicylic acid-mediated defense against *Pseudomonas syringae*. *Phytochemistry* 112: 110-121

Marino D, Andrio E, Danchin EG, Oger E, Gucciardo S, Lambert A, Puppo A, Pauly N (2011) A *Medicago truncatula* NADPH oxidase is involved in symbiotic nodule functioning. *New Phytol* 189:580–592

Marino D, Dunand C, Puppo A, Pauly N. 2012. A burst of plant NADPH oxidases. *Trends in Plant Science* 17, 9–15.

Marquez-Villavicencio Mdel P, Weber B, Witherell RA, Willis DK, Charkowski AO. (2011). The 3-hydroxy-2-butanone pathway is required for *Pectobacterium carotovorum* pathogenesis. *PLoS One* 6: e22974.

Martinez C, Montillet J, Bresson E, Agnel JP, Dai GH, Daniel JF, Geiger JP, Nicole M (1998) Apoplastic peroxidase generates superoxide anions in cells of cotton cotyledons undergoing the hypersensitive reaction to *Xanthomonas campestris* pv.

malvacearum Race 18. *Mol Plant Microbe Interact* 11:1038–1047

Matsui H, Nomura Y, Egusa M, Hamada T, Hyon GS, Kaminaka H, Watanabe Y, Ueda T, Trujillo M, Shirasu K, Nakagami H (2017) The GYF domain protein PSIG1 dampens the induction of cell death during plant-pathogen interactions. *PLoS Genet* 13(10): e1007037

Medzhitov R, Preston-Hurlburt P, Janeway CA Jr (1997) A human homologue of the *Drosophila* Toll protein signals activation of adaptive immunity. *Nature* 388:394–397

Mehdy MC (1994) Active oxygen species in plant defense against pathogens. *Plant Physiol* 105:467–472

Melotto M, Underwood W, He SY. (2008). Role of stomata in plant innate immunity and foliar bacterial diseases. *Annu. Rev. Phytopathol.* 46: 101–22

Münch S., Lingner U., Floss D.S., Ludwig N., Sauer N., Deising H.B. The hemibiotrophic lifestyle of *Colletotrichum* species. *J. Plant Physiol.* 2008; 165:41–51.

Nakagawa T, Kurose T, Hino T, Tanaka K, Kawamukai M, Niwa Y, Toyooka K, Matsuoka K, Jindo T, Kimura T. (2017) Development of series of gateway binary vectors, pGWBs, for realizing efficient construction of fusion genes for plant transformation. *J Biosci Bioeng* 104: 34-41

Narusaka M., Abe H., Kobayashi M., Kubo Y., Narusaka Y. Comparative analysis of expression profiles of counterpart gene sets between *Brassica rapa* and *Arabidopsis thaliana* during fungal pathogen *Colletotrichum higginsianum* infection. *Plant Biotechnol. J.* 2006; 23:503–508.

Nishinaka Y, Aramaki Y, Yoshida H, Masuya H, Sugawara T, Ichimori Y. (1993) A

new sensitive chemiluminescence probe, L-012, for measuring the production of superoxide anion by cells. *Biochem Biophys Res Commun.* 193(2):554-9.

Nühse TS, Bottrill AR, Jones AME, Peck SC (2007) Quantitative phosphoproteomic analysis of plasma membrane proteins reveals regulatory mechanisms of plant innate immune responses. *Plant J* 51:931–940

O'Brien JA, Daudi A, Butt VS, Bolwell GP (2012a) Reactive oxygen species and their role in plant defence and cell wall metabolism. *Planta* 236: 765-779

O'Brien JA, Daudi A, Finch P, Butt VS, Whitelegge JP, Souda P, Ausubel FM, Bolwell GP (2012b) A peroxidase-dependent apoplastic oxidative burst in cultured *Arabidopsis* cells functions in MAMP-elicited defense. *Plant Physiol* 158: 2013-2027

Ogasawara Y, Kaya H, Hiraoka G, Yumoto F, Kimura S, Kadota Y, Hishinuma H, Senzaki E, Yamagoe S, Nagata K, Nara M, Suzuki K, Tanokura M, Kuchitsu K (2008) Synergistic activation of the *Arabidopsis* NADPH oxidase *AtrbohD* by  $Ca^{2+}$  and phosphorylation. *J Biol Chem* 283:8885–8892

Oliva M, Theiler G, Zamocky M, Koua D, Margis-Pinheiro M, Passardi F, Dunand C (2009) PeroxiBase: a powerful tool to collect and analyse peroxidase sequences from Viridiplantae. *J Exp Bot* 60: 453-459

Passardi F, Longet D, Penel C, Dunand C. The class III peroxidase multigenic family in rice and its evolution in land plants, *Phytochemistry*, 2004, vol. 65 (pg. 1879-1893)

Passardi F, Tognolli M, Meyer MD, Penel C, 276 Dunand C (2006) Two cell wall associated peroxidases from *Arabidopsis* influence root elongation. *Planta* 223: 965-974

Passardi F, Zamocky M, Favet J, Jakopitsch C, Penel C, Obinger C, Dunand C (2007) Phylogenetic distribution of catalase-peroxidases: are these patches of order in chaos? *Gene*. 397, 101-113

Peng M, Kuc J (1992) Peroxidase-generated hydrogen peroxide as a source of antifungal activity in vitro and on tobacco leaf disks. *Phytopathology* 82:696–699

Poltorak A, He X, Smirnova I, Liu MY, Van Huffel C, Du X, Birdwell D, Alejos E, Silva M, Galanos C, Freudenberg M, Ricciardi-Castagnoli P, Layton B, Beutler B (1998) Defective LPS signaling in C3H/HeJ and C57BL/10ScCr mice: mutations in Tlr4 gene. *Science* 282:2085–2088

Qiu X, Lei C, Huang L, Li X, Hao H, Du Z, Wang H, Ye H, Beerhues L, Liu B (2012) Endogenous hydrogen peroxide is a key factor in the yeast extract-induced activation of biphenyl biosynthesis in cell cultures of *Sorbus aucuparia*. *Planta* 235:217–223

Radhamony, R.N. A.M. Prasad. and R. Srinivasan, R. (2005) T-DNA insertional mutagenesis in *Arabidopsis*: a tool for functional genomics. *E. Journal Biotechnology* 8: 1-20.

Ravensdalea M, Blom TJ, Gracia-Garza JA, Svircev AM, Smithc RJ. (2007). Bacteriophages and the control of *Erwinia carotovora* subsp. *carotovora*. *Can. J. Plant Pathol.* 29: 121-130.

Raymond J, Segré D. 2006. The effect of oxygen on biochemical networks and the evolution of complex life. *Science* 311:1764–6

Schwessinger B, Ronald PC (2012) Plant innate immunity: Perception of conserved microbial signatures. *Annu Rev Plant Biol* 63:451–482

Schwessinger B, Zipfel C (2008) News from the frontline: recent insights into PAMP-triggered immunity in plants. *Curr Opin Plant Biol* 11:389–395

Shigeto J, Tsutsumi Y (2016) Diverse functions and reactions of class III peroxidases. *New Phytol* 209: 1395-1402

Shimada C., Lipka V., O’Connell R., Okuno T., Schulze-Lefert P., Takano Y. Nonhost resistance in Arabidopsis-Colletotrichum interactions acts at the cell periphery and requires actin filament function. *Mol. Plant-Microbe Interact.* 2006; 19:270–279.

Sohn HY, Gloe T, Keller M, Schoenafinger K, Pohl U. (1999) Sensitive superoxide detection in vascular cells by the new chemiluminescence dye L-012. *J Vasc Res.* 36:456–464.

Song WY, Wang GL, Chen LL, Kim HS, Pi LY, Holsten T, Gardner J, Wang B, Zhai WX, Zhu LH, Fauquet C, Ronald P (1995) A receptor kinase-like protein encoded by the rice disease resistance gene, Xa21. *Science* 270:1804–1806

Staats, M., Van Baarlen, P. and Van Kan, J.A.L. (2005) Molecular phylogeny of the plant pathogenic genus *Botrytis* and the evolution of host specificity. *Mol. Biol. Evol.* 22, 333–346.

Staats, M., Van Baarlen, P., Schouten, A., Van Kan, J.A.L. and Bakker, F.T. (2007) Positive selection in phytotoxic protein-encoding genes of *Botrytis* species. *Fungal Genet. Biol.* 44, 52–63.

Sumimoto H. (2008). Structure, regulation and evolution of Nox-family NADPH oxidases that produce reactive oxygen species. *FEBS Journal* 275, 3249–77.

Sutherland MW (1991) The generation of oxygen radicals during host plant responses to infection. *Physiol Mol Plant Pathol* 39:79–93

Suzuki N, Miller G, Morales J, Shulaev V, Torres MA, Mittler R (2011) Respiratory burst oxidases: the engines of ROS signaling. *Curr Opin Plant Biol* 14:691–699

Thordal-Christensen H, Zhang Z, Wei Y, Collinge DB (1997) Subcellular localization of H<sub>2</sub>O<sub>2</sub> in plants. H<sub>2</sub>O<sub>2</sub> accumulation in papillae and hypersensitive response during the barley–powdery mildew interaction. *Plant J* 11:1187–1194

Tognolli M, Penel C, Greppin H, Simon P (2002) Analysis and expression of the class III peroxidase large gene family in *Arabidopsis thaliana*. *Gene* 288: 129-138

Torres MA, Dangl JL (2005) Functions of the respiratory burst oxidase in biotic interactions, abiotic stress and development. *Curr Opin Plant Biol* 8:397–403

Torres MA, Dangl JL, Jones JDG (2002) *Arabidopsis* gp91phox homologues AtrbohD and AtrbohF are required for accumulation of reactive oxygen intermediates in the plant defense response. *Proc Natl Acad Sci USA* 99:517–522

Torres MA, Jones JD, Dangl JL (2006) Reactive oxygen species signaling in response to pathogens. *Plant Physiol* 141:373–378

Toyoda K, Yasunaga E, Niwa M, Ohwatari Y, Nakashima A, Inagaki Y, Ichinose Y, Shiraishi T (2012) H<sub>2</sub>O<sub>2</sub> production by copper amine oxidase, a component of the ecto-apyrase (ATPase)-containing protein complex(es) in the pea cell wall, is regulated by an elicitor and a suppressor from *Mycosphaerella pinodes*. *J Gen Plant Pathol* 78, 311-315

Tsuda, K., and Katagiri, F. (2010). Comparing signaling mechanisms engaged in

pattern-triggered and effector-triggered immunity. *Curr. Opin. Plant Biol.* 13, 459–465.

Welinder KG, Justesen AF, Kjaersgård IV, Jensen RB, Rasmussen SK, Jespersen HM, Duroux L (2002) Structural diversity and transcription of class III peroxidases from *Arabidopsis thaliana*, *European Journal of Biochemistry.* 269, 6063-6081

Welinder KG, Justesen AF, Kjærsgård IVH, Jensen RB, Rasmussen SK, Jespersen HM, Duroux L (2002) Structural diversity and transcription of class III peroxidases from *Arabidopsis thaliana*. *FEBS J* 269: 6063-6081

Whalen, M. C., Innes, R. W., Bent, A. F., and Staskawicz, B. J. (1991). Identification of *Pseudomonas syringae* pathogens of *Arabidopsis* and a bacterial locus determining avirulence on both *Arabidopsis* and soybean. *Plant Cell* 3:49-59.

Whitehead NA, Byers JT, Commander P, Corbett MJ, Coulthurst SJ, Everson L, et al. 2002. The regulation of virulence in phytopathogenic *Erwinia* species: quorum sensing, antibiotics and ecological considerations. *Antonie Van Leeuwenhoek* 81: 223-231.

Williamson B, Tudzynski B, Tudzynski P, van Kan JA. (2007) *Botrytis cinerea*: the cause of grey mould disease. *MOLECULAR PLANT PATHOLOGY* (2007) 8 (5), 561–580

Wojtaszek P (1997) Oxidative burst: an early plant response to pathogen infection. *Biochem J* 322(Pt 3):681–692

Wojtaszek P, Trethowan J, Bolwell GP (1995) Specificity in the immobilisation of cell wall proteins in response to different elicitor molecules in suspension-cultured

cells of French bean (*Phaseolus vulgaris* L.). *Plant Mol Biol* 28:1075–1087

Zipfel C, Kunze G, Chinchilla D, Caniard A, Jones JDG, Boller T, Felix G (2006)

Perception of the bacterial PAMP EF-Tu by the receptor EFR restricts

*Agrobacterium*-mediated transformation. *Cell* 125:749–760

Zipfel, C. (2008). Pattern-recognition receptors in plant innate immunity. 20, 10–16.

Zipfel, C. (2009). Early molecular events in PAMP-triggered immunity. *Curr. Opin.*

*Plant Biol.* 12, 414–420.

Zipfel, C. (2014). Plant pattern-recognition receptors. *Trends Immunol.* 35, 345–351.

# Acknowledgements

The first and foremost I wish to sincerely thank my chief supervisor Professor, Dr. Kazuhiro Toyoda for his constant encouragement, intellectual guidance and valuable assistance throughout the study period and for providing me with the best study environment to carry out my research. I will forever be grateful for his support in academics and beyond.

I would like to extend my sincere gratitude to my co-supervisor Assoc. Prof. Dr. Yoshiteru Noutoshi and Prof. Dr. Yuki Ichinose for their kind assistance and academic advice during my studies and research. Special thanks to Dr. Hirofumi Nakagami for his valuable advice and critical comments on the thesis.

I am grateful to Dr. Hidenori Matsui facilitating the accomplishment of this study through your valuable discussion, suggestions and technique help.

Thanks to Associate Professor Mikihiro Yamamoto. The advice from seminar was most helpful.

Special thanks should go to Mai Thanh Luan, Le Thi Phuong, Aprilia Nur Fitrianti, Matsuo Mika, Takasu Mizuho, Yamasaki Shiori and Kawabata Maya for their guidance, help, encouragement and supports. My acknowledgement also goes to all the students from the Phytopathology laboratory and Genetic Engineering laboratory for their valuable suggestion and their friendliness giving me a wonderful memory of my doctoral course. Without them, this thesis would not have been the same as presented here.

I am deeply indebted to my mother and wife for their love and continued support during my pursuit of education over the years.